Antibody Evolution after SARS-CoV-2 mRNA Vaccination

Alice Cho[1,*], Frauke Muecksch[2,*], Dennis Schaefer-Babajew[1,*], Zijun Wang[1,*], Shlomo Finkin[1,*],Christian Gaebler[1], Victor Ramos[1], Melissa Cipolla[1], Marianna Agudelo[1], Eva Bednarski[2], Justin DaSilva[2], Irina Shimeliovich[1], Juan Dizon[1], Mridushi Daga[1], Katrina Millard[1], Martina Turroja[1], Fabian Schmidt[2], Fengwen Zhang[2], Tarek Ben Tanfous[1], Mila Jankovic[1], Thiago Y. Oliveria[1], Anna Gazumyan[1], Marina Caskey[1], Paul D. Bieniasz[2,3], Theodora Hatziioannou[2], and Michel C. Nussenzweig[1,3].

[1]Laboratory of Molecular Immunology, The Rockefeller University, New York, NY 10065, USA

[2]Laboratory of Retrovirology, The Rockefeller University, New York, NY 10065, USA

[3]Howard Hughes Medical Institute

*equal contribution

Address correspondence to: Paul D. Bieniasz pbieniasz@rockefeller.edu; Marina Caskey mcaskey@rockefeller.edu; Theodora Hatziioannou thatziio@rockefeller.edu; or Michel C. Nussenzweig nussen@rockefeller.edu

Summary

Severe acute respiratory syndrome coronavirus 2 (SARS-CoV-2) infection produces B-cell responses that continue to evolve for at least one year. During that time, memory B cells express increasingly broad and potent antibodies that are resistant to mutations found in variants of concern[1]. As a result, vaccination of coronavirus disease 2019 (COVID-19) convalescent individuals with currently available mRNA vaccines produces high levels of plasma neutralizing activity against all variants tested[1,2]. Here, we examine memory B cell evolution 5 months after vaccination with either Moderna (mRNA-1273) or Pfizer-BioNTech (BNT162b2) mRNA vaccines in a cohort of SARS-CoV-2 naïve individuals. Between prime and boost, memory B cells produce antibodies that evolve increased neutralizing activity, but there is no further increase in potency or breadth thereafter. Instead, memory B cells that emerge 5 months after vaccination of naïve individuals express antibodies that are equivalent to those that dominate the initial response. We conclude that memory antibodies selected over time by natural infection have greater potency and breadth than antibodies elicited by vaccination. These results suggest that boosting vaccinated individuals with currently available mRNA vaccines would produce a quantitative increase in plasma neutralizing activity but not the qualitative advantage against variants obtained by vaccinating convalescent individuals.

Between January 21 and June 23, 2021, we recruited 32 volunteers with no history of prior SARS-CoV-2 infection receiving either Moderna (mRNA-1273; n=8) or Pfizer-BioNTech (BNT162b2; n=24) mRNA vaccines for sequential blood donation. Matched samples were obtained an average of 2.5 and 5 weeks after the prime and boost, respectively, and an additional

42 set of matched samples an average of 2 and 5 months after the boost. The volunteers ranged in
43 age from 23-78 years (median 34.5 years), 53% were male and 47% female (for details see
44 Methods and Supplementary Tables 1 and 2).
45
46 **Plasma binding and neutralization assays**
47 Plasma IgM, IgG, and IgA responses to SARS-CoV-2 receptor binding domain (RBD) were
48 measured by enzyme linked immunosorbent assay (ELISA)[3]. As reported by others[2,4-6] there was
49 a significant increase in IgG reactivity to RBD between prime and boost ($p<0.0001$, Fig. 1a).
50 IgM and IgA titers were lower than IgG titers and remained low after the second vaccine dose
51 (Extended data Fig. 1a and b). The magnitude of the response was inversely correlated with age
52 after the prime ($r=-0.54$, $p=0.005$), but the difference was no longer significant after the boost
53 (Fig. 1b). Between 2 and 5 months after the boost, anti-RBD titers of all isotypes decreased
54 significantly. IgG titers decreased by an average of 5.2-fold (range: 2.1- to 10.2-fold) and the
55 loss of activity was directly correlated to the time after vaccination ($p<0.0001$, Fig. 1c and d and
56 Extended data Fig. 1c and d).
57
58 Neutralizing activity was measured using HIV-1 pseudotyped with the SARS-CoV-2 spike[1,3,7,8].
59 Naïve individuals showed variable responses to the initial vaccine dose with a geometric mean
60 half-maximal neutralizing titer (NT_{50}) of 171 (Fig. 1e and Supplementary Table 2). The
61 magnitude of the neutralizing responses to the initial vaccine dose in naïve volunteers was
62 inversely correlated with age ($r=-0.39$, $p=0.05$, Fig. 1f). Both binding and neutralizing responses
63 to the second vaccine dose were correlated to the prime ($r=0.46$, $p=0.02$, Extended data. Fig. 1e;
64 $r=0.54$, $p=0.003$, Extended data Fig. 1f) and produced a nearly 15-fold increase in the geometric

65 mean neutralizing response that was similar in males and females and eliminated the age-related
66 difference in neutralizing activity (Extended data 2g and Fig. 1f). After the boost naïve vaccinees
67 had 6.2-fold higher neutralizing titers than a cohort of infected individuals measured 1.3 months
68 after symptom onset[3] ($p<0.0001$, Fig. 1e). Neutralizing responses were directly correlated to IgG
69 anti-RBD titers ($r=0.96$, $p<0.0001$, Fig. 1g). Thus, the data obtained from this cohort agree with
70 prior observations showing a significant increase in plasma neutralizing activity that are
71 correlated with improved vaccine efficacy in naïve individuals that receive the second dose of
72 mRNA vaccine[2,6,9,10].
73
74 The 15 individuals assayed 5 months after vaccination had an average 4.7-fold decrease in
75 geometric mean neutralizing activity from their 2-month measurement ($p=0.04$, Fig. 1h), with a
76 range of 1.4- to 27-fold (Fig. 1i). Neutralizing activity was inversely correlated with the time
77 from vaccination ($r=-0.75$, $p<0.0001$, Fig. 1j), and directly correlated to IgG anti-RBD binding
78 titers when assessed 5 months after vaccination (Extended data. Fig. 1h).
79
80 We and others showed that the neutralizing responses elicited by mRNA vaccination are more
81 potent against the original Wuhan Hu-1 strain than for some of the currently circulating variants
82 of concern[2,11-13]. To confirm these observations, we measured the neutralizing activity of the
83 paired plasmas from naive individuals 2 and 5 months after the second vaccine dose against
84 B.1.1.7 (alpha variant), B.1.351 (beta variant), B.1.526 (first isolated in New York City), P.1
85 (gamma variant) and B.1.617.2 (delta variant). Consistent with previous reports[12,14-16] the
86 neutralizing activity against the variants was lower than against the original Wuhan Hu-1 strain
87 (Fig. 1k, Supplementary Table 3). Initial geometric mean neutralizing titers at 2 months against

88 B.1.351, B.1.1.7, B.1.526, P.1 and B.1.617.2 were 5.7, 1.8, 1.1, 1.4 and 2.7-fold lower than
89 against Wuhan-Hu respectively (Fig. 1k). In the months following vaccination there was a
90 decrease in neutralizing activity against all variants that paralleled the drop in activity against
91 Wuhan Hu-1 (R683G) with geometric mean neutralizing titers for WT, B.1.351, B.1.1.7,
92 B.1.526, P.1 and B.1.617.2 decreasing by 2.9-, 1.8-, 2.3-, 2.9-, 2.4- and 2.6-fold, respectively
93 (Fig. 1k and Supplementary Table 3). Nevertheless, vaccine-induced neutralizing activity at 5
94 months against all variants exceeds Wuhan-Hu plasma neutralization of convalescent individuals
95 after 6.2 months.
96
97
98 **Monoclonal Antibodies**
99 Circulating antibodies produced by plasma cells can prevent infection if present at sufficiently
100 high concentrations at the time of exposure. In contrast, the memory B cell compartment
101 contains long lived antigen-specific B cells that mediate rapid recall responses that contribute to
102 long term protection[17]. To examine the nature of the memory compartment elicited by one or two
103 mRNA vaccine doses and its evolution after 5 months we used flow cytometry to enumerate B
104 cells expressing receptors that bind to Wuhan Hu-1 (wild type) and the B.1.351
105 K417N/E484K/N501Y (KEN) variant RBDs (Fig. 2a and b, and Extended data Fig. 2). Wuhan-
106 Hu RBD-specific memory B cells developed after the prime in all volunteers examined and their
107 numbers increased for up to 5 months after vaccination (Fig. 2a). Memory B cells binding to the
108 B.1.351 RBD were detectable but in lower numbers than wild type RBD-binding B cells in all
109 samples examined (Fig. 2b). Whereas IgG memory cells increased after the boost, IgM-
110 expressing memory B cells that made up 23% of the memory compartment after the prime were

111 nearly absent after boosting (Fig. 2c). Finally, circulating RBD-specific plasmablasts were
112 readily detected after the prime but were infrequent after the boost (Fig. 2d, and Extended data
113 Fig. 2d).
114
115 The memory compartment continues to evolve up to one year after natural infection with
116 selective enrichment of cells producing broad and potent neutralizing antibodies[1]. To determine
117 how the memory compartment evolves after vaccination, we obtained 1524 paired antibody
118 sequences from 6 individuals sampled at 2.5 weeks after prime and 5 weeks or 5 months after
119 boost, and an additional 804 paired antibody sequences from 5 individuals sampled after 2- or 5-
120 months after boost (Fig. 2e and f, Extended Data Fig 3, Supplementary Table 4). As expected
121 *IGHV3-30* and *IGHV3-53* were over-represented after the first and second vaccine dose and
122 remained over-represented 5 months after vaccination[18-20] (Extended data Fig. 4).
123
124 All individuals examined showed expanded clones of memory B cells that expressed closely
125 related IGHV and IGHL genes (Fig. 2e and f, Extended data Fig. 4). Paired prime and boost
126 samples showed expanded clones of memory B cells some of which were shared across
127 plasmablast, IgM and IgG prime, and IgG boost memory cells (Extended data Fig. 3 and 5).
128 Thus, the cell fate decision controlling the germinal center versus plasmablast decision is not
129 entirely affinity dependent since cells with the same initial affinity can enter both
130 compartments[21].
131
132 The relative fraction of memory cells found in expanded clones varied between prime and boost
133 and between individuals (Fig. 2e). However, new clones that develop after the boost represent a

134 greater fraction (80%) of the total clones than the conserved clones in all individuals (Fig. 2e).
135 Finally, memory B cells emerging after the boost showed significantly higher levels of somatic
136 mutations than plasmablasts or memory B cells isolated after the prime (Extended data Fig. 3b).
137
138 After 5 months, there was an overall decrease in the percentage of clones in the RBD-binding
139 memory compartment (Fig. 2g). Nevertheless, clones of memory B cells continued to evolve for
140 up to 5 months in vaccinated individuals as evidenced by the dominance of newly emerging
141 clones (86%, Fig. 2e and f) and the significant increase in somatic mutation between the time
142 points ($p<0.0001$, Fig. 2h, Extended data Fig. 3c). The number of mutations in antibody genes
143 was comparable between vaccinated and convalescent individuals after 5 months (Fig. 2h,
144 Extended data Fig. 3c). In conclusion the memory B cell compartment continues to evolve for up
145 to 5 months after mRNA vaccination.
146
147 **Neutralizing Activity of Monoclonal Antibodies**
148 We performed ELISAs to confirm that the antibodies isolated from memory B cells bind to RBD
149 (Extended data Fig. 6). 403 antibodies were tested by ELISA including: 86 isolated after the first
150 vaccine dose; 92 isolated after the second vaccine dose; 111 isolated 2 months after the second
151 vaccine dose and 114 isolated from individuals that had been fully vaccinated 5 months earlier.
152 Among the 403 antibodies tested 381 (95%) bound to the Wuhan Hu-1 RBD indicating that the
153 method used to isolate RBD-specific memory B cells was highly efficient (Supplementary Table
154 5-7). The geometric mean ELISA half-maximal concentration (EC_{50}) of the antibodies obtained
155 after prime, boost, 2 months and 5 months was 3.9, 2.6, 3.2 and 2.8 ng/ml respectively,
156 suggestive of no change in binding over time after vaccination (Extended data Fig. 6 and

157 Supplementary Table 5). Binding among all antibodies did not improve between prime and
158 boost, or 2 and 5 months (Extended data Fig. 6). However, a slight improvement was observed
159 after 5 months among clones (Extended data Fig.6).
160
161 381 RBD-binding antibodies were tested for neutralizing activity using HIV-1 pseudotyped with
162 the SARS-CoV-2 spike[3,8]. The geometric mean half-maximal inhibitory concentration (IC_{50}) of
163 the RBD-specific memory antibodies improved from 380 ng/ml to 170 ng/ml between the first
164 and second vaccine dose (p=0.005, Fig. 3a). The improvement was reflected in all clones (IC_{50}
165 370 vs. 182 ng/ml, p=0.03 Fig. 3b), newly arising clones (IC_{50} 430 vs. 165 ng/ml, p=0.02 Fig.
166 3c), single antibodies (IC_{50} 357 vs. 131 ng/ml, Fig. 3d) and conserved clones (IC_{50} 314 vs. 208
167 ng/ml, Fig. 3e, Supplementary Table 6). The increase in neutralizing activity between the first
168 and second vaccine dose was associated with a decrease in the percentage of non-neutralizing
169 antibodies (defined as IC50 >1000ng/ml) and increased representation of neutralizing antibodies
170 (p= 0.03, Fig. 3a). In conclusion, memory B cells recruited after the boost account for most of
171 the improvement in neutralizing activity in this compartment between the 2 vaccine doses. Thus,
172 in addition to the quantitative improvement in serum neutralizing activity there is a qualitative
173 improvement in the memory compartment after boosting.
174
175 There was no further improvement in neutralizing activity of the monoclonal antibodies obtained
176 between 2 and 5 months after vaccination (IC_{50} 140 vs. 144 ng/ml, Fig. 3f). This was true when
177 considering all B cell clones, newly arising clones or single memory B cells separately (Fig. 3g-j,
178 Supplementary table 7). In contrast, memory antibodies obtained from convalescent individuals
179 showed improved neutralizing activity between 1.3[3] and 6.2 months[7] with IC_{50} of 171 ng/ml to

180 116 ng/ml (Fig. 3f), which improved further after 1 year[1]. This improvement was due to
181 increased neutralizing activity among persisting clones (p=0.003, Fig. 3h).
182
183 **Affinity, Epitopes and Neutralization Breadth**
184 To examine affinity maturation after vaccination, we performed biolayer interferometry (BLI)
185 experiments using the Wuhan Hu-1 RBD[3]. 60 randomly selected antibodies were assayed from
186 the prime-boost cohort, 30 obtained after the prime and 30 after the boost, with similar overall
187 geometric mean IC_{50}s ranging from <10 ng/ml to >1000 ng/ml (Extended data Fig. 7a). There
188 was no significant difference in affinity between the antibodies obtained after the prime and
189 boost, and no correlation between affinity and neutralizing activity (Fig. 4a and Extended Data
190 Fig. 7 b and c). Similar experiments were performed on 31 and 30 antibodies obtained from the
191 2- and 5-month time points from vaccinated individuals, respectively. Despite similar levels of
192 neutralizing activity (Extended data Fig. 7d), there was an average 2.6-fold increase in the
193 affinity of the antibodies obtained between 2 and 5 months after vaccination (p=0.02, Fig. 4b and
194 Extended Data Fig. 7e and f).
195
196 We also compared the affinities of pairs of antibodies obtained from conserved clones between 2
197 and 5 months after vaccination. Conserved clones obtained at 2 and 5 months from vaccinated
198 individuals showed an average 1.9-fold increase in affinity (p=0.03, Fig. 4c). In contrast, a
199 comparable group of conserved clonal antibodies obtained from convalescent individuals 1.3 and
200 6.2 months after infection showed an average 24-fold increase in affinity (p=0.002, Fig. 4c).
201

202 In addition to the increase in potency, the neutralizing breath of memory antibodies obtained
203 from conserved clones from convalescent individuals increases with time after infection[1,7,22]. To
204 determine whether there is a similar increase in breadth with time after vaccination, we selected
205 20 random antibodies from the prime or boost, with representative levels of activity against the
206 original Wuhan Hu-1 strain, and measured their neutralization potency against a panel of
207 psudotypes encoding RBD mutations associated with circulating variants of concern (Extended
208 data. Fig. 8). There was little change in breadth between prime and boost, with only a small
209 increase in resilience to K417N and A475V substitutions (Extended data Fig. 8, Supplementary
210 Table 8).
211
212 In addition, we assayed 10 conserved pairs of neutralizing antibodies obtained 2 and 5 months
213 after vaccination against the same RBD mutant pseudotypes (Fig. 4d and Supplementary Table
214 9). They were compared to 6 previously reported[22], plus 10 additional pairs of antibodies
215 obtained from convalescent individuals at 1.3- and 6.2-month time points (Fig. 4e and
216 Supplementary Table 9). Whereas only 4 of 10 of the vaccine antibodies showed improved
217 breadth, 15 of the 16 convalescent pairs developed increased breadth. Moreover, only 1 of the 10
218 vaccine antibody pairs showed improved potency against pseudotypes carrying B.1.617.2 (delta
219 variant)-specific RBD amino acid substitutions (L452R/T478K), while 11 out of 16 convalescent
220 antibody pairs showed improved activity against this virus (Fig. 4d and e). We conclude that
221 antibody evolution differs in convalescent and vaccinated individuals in that there is less affinity
222 maturation and little increase in breadth between 2 and 5 months after mRNA vaccination.
223

224 Circulating antibodies are produced by plasma cells with variable longevity[23-26]. SARS-CoV-2
225 infection or mRNA vaccination produces an early peak antibody response that decreases by 5-
226 10-fold after 5 months[7,27-31]. Notably, peak neutralization titres after vaccination exceed those of
227 COVID-19 recovered individuals. Nevertheless, neutralizing potency against variants is
228 significantly lower than against Wuhan Hu-1, with up to 5-10-fold reduced activity against the
229 B.1.351 variant[5,6,12,13,32]. Taken together with the overall decay in neutralizing activity there can
230 be 1-2 orders of magnitude decrease in serum neutralizing activity after 5 or 6 months against
231 variants when compared to the peak of neutralizing activity against Wuhan Hu-1. Thus, antibody
232 mediated protection against variants is expected to wane significantly over a period of months,
233 consistent with reports of reinfections in convalescent individuals and breakthrough infection by
234 variants in fully vaccinated individuals[33-35].
235
236 In contrast to circulating antibodies, memory B cells are responsible for rapid recall responses[36-
237 39], and this compartment is relatively stable over the first 6 months after natural infection[7,40] or
238 mRNA vaccination. In both cases memory B cells continue to evolve for up to 5 months as
239 evidenced by increasing levels of somatic mutation and emergence of newly expanded clones.
240
241 The memory response would be expected to protect individuals that suffer breakthrough
242 infection from developing serious disease. However, memory B cell evolution differs in
243 important ways between infection and mRNA vaccination. Both natural infection and mRNA
244 vaccination produce memory antibodies that evolve increased affinity, but the increase in affinity
245 is more modest after vaccination. This difference is consistent with the observation that vaccine-

246 elicited memory antibodies fail to show the increased neutralizing breadth that developed after
247 natural infection[1,7].
248
249 There are innumerable differences between natural infection and mRNA vaccination that could
250 account for the differences in antibody evolution over time. These include but are not limited to:
251 1. Route of antigen delivery, respiratory tract vs. intra-muscular injection[41,42]; 2. The physical
252 nature of the antigen, intact virus vs. S protein[43]; 3. Antigen persistence, weeks in the case of
253 natural infection[7] vs. hours to days for mRNA[44]. Each of these could impact on B cell evolution
254 and selection directly, and indirectly through differential T cell recruitment.
255
256 The increase in potency and breadth in the memory compartment that develops after natural
257 infection accounts for the exceptional responses to Wuhan Hu-1 and its variants that
258 convalescent individuals develop when boosted with mRNA vaccines[1,5]. The expanded memory
259 B cell compartment in mRNA vaccinees should also produce high titers of neutralizing
260 antibodies but with decreased breath in comparison to natural infection when vaccinees are
261 boosted or when they are re-exposed to the virus[45].Thus, boosting vaccinated individuals with
262 currently available mRNA vaccines will produce strong responses that mirror their initial vaccine
263 responses to Wuhan-Hu with similarly decreased coverage against variants. Finally, timing a
264 boost for optimal responses will depend on whether the objective is to prevent viral acquisition
265 or disease[46]. Given the rapid emergence of variants, in the former, boosting would be needed on
266 a far shorter time scale than the latter. The optimal timing for boosting to prevent serious disease
267 will depend on the stability and further evolution of the memory B cell compartment.
268

269 **FIGURES**

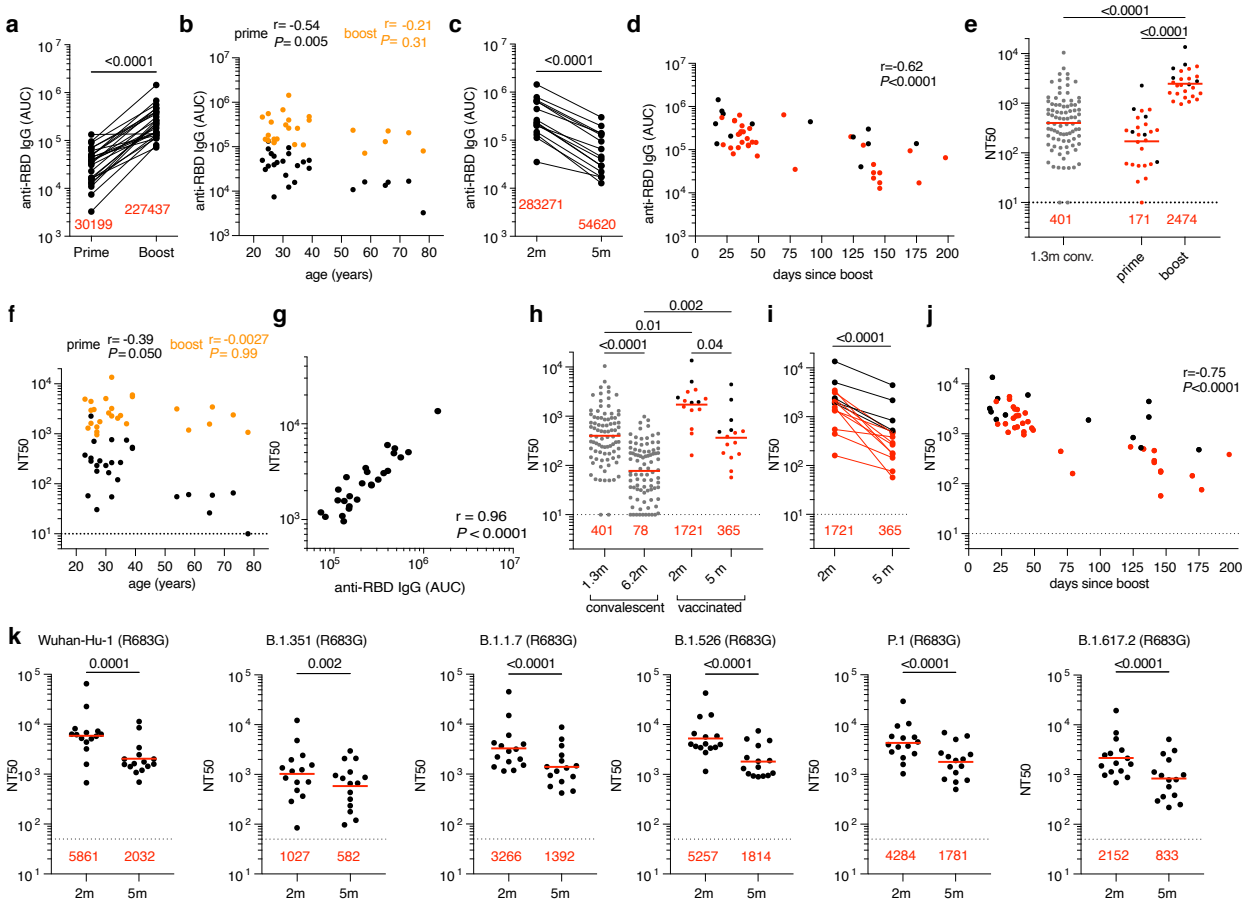

270

271 **Fig. 1: Plasma ELISAs and neutralizing activity.**

272 **a,** Graph shows area under the curve (AUC, Y-axis) for plasma IgG antibody binding to SARS-
273 CoV-2 RBD after prime and boost for paired samples. (n=26) **b**, Graph shows plasma IgG antibody
274 binding (AUC, Y-axis) plotted against age (X-axis) after prime (black) and boost (orange). **c**,
275 Graph shows AUC (Y-axis) for plasma IgG antibody binding to SARS-CoV-2 RBD for paired
276 samples obtained 2 and 5 months after the boost. (n=15) **d,** Graph shows AUC values from **a**, and
277 **b,** (Y-axis) plotted against time after vaccination (X-axis). **e,** NT50 in convalescent individuals
278 1.3m after infection[3] and in vaccinated individuals after 1 dose (prime) or 2 doses (boost) of an
279 mRNA vaccine. **f**, NT50 values (Y-axis) vs. age (years X-axis) in individuals receiving 1 dose
280 (prime, black) or two doses (boost, orange) of an mRNA vaccine. **g**, NT50 values (Y-axis) vs. IgG

281 antibody binding (AUC, X-axis) after boost in individuals receiving two doses of an mRNA
282 vaccine. **h**, NT50 values in convalescent individuals 1.3m[3] and 6.2m[7] after infection and in
283 vaccinated individuals 2- [12] and 5-months (m) after receiving 2 doses of an mRNA vaccine. **i,**
284 NT50 values in vaccinated individuals 2-[12] and 5-months after receiving 2 doses of an mRNA
285 vaccine. Lines connect paired longitudinal samples from the same individual. **j**, Graph shows
286 NT50 values (Y-axis) vs. days (X-axis) after boost in individuals receiving two doses of an mRNA
287 vaccine. **k**, Plasma neutralizing activity against indicated SARS-CoV-2 variants of concern (n=15
288 paired samples at 2- and 5-months after full vaccination). Refer to Methods for a list of all
289 substitutions/deletions/insertions in the spike variants. All experiments were performed at least in
290 duplicate. NT50 values for Moderna mRNA-1273 and Pfizer-BioNTech BNT162b2 in **d, e, h-j**
291 are shown in black and red, respectively. Red bars and values in **e, h,** and **k** represent geometric
292 mean NT50 values. Statistical significance in **a, c, i** and **k** was determined by Wilcoxon test, in **b,**
293 **d, f, g** and **j** by spearman correlation test and in **e** and **h** by Kruskal-Wallis test with subsequent
294 Dunn's multiple comparisons.
295

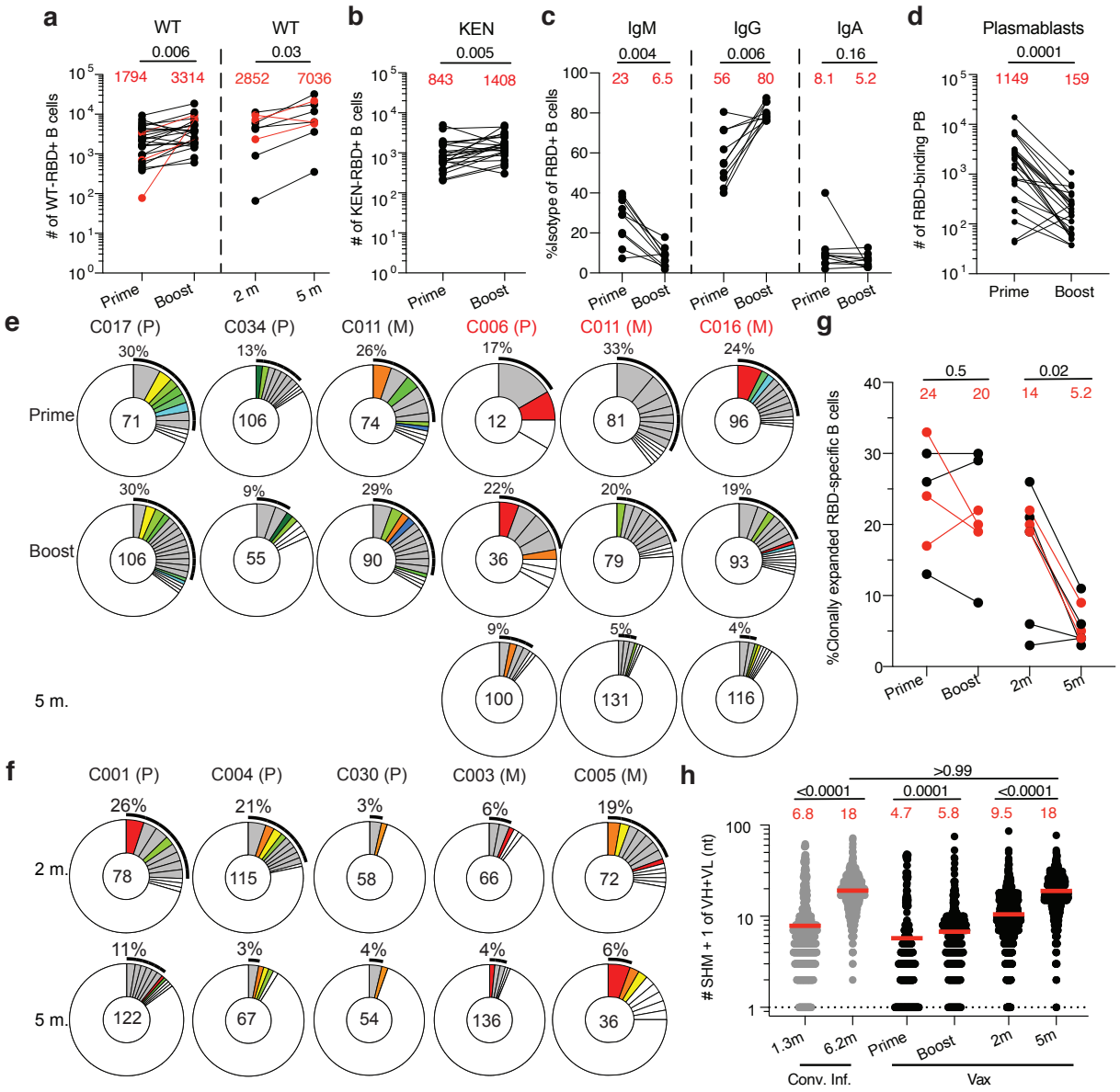

Fig. 2: Anti-SARS-CoV-2 RBD B cells after vaccination. a-d, Graphs summarizing **a,** the number of Wuhan-Hu RBD (WT)-specific memory B cells per 10 million B cells for vaccinees after prime or boost (n=26) or at follow-up of 2-[12] and 5-months after full vaccination (n=9), including 3 individuals who were sampled at prime, boost, and again 5 months post-vaccination (illustrated by red dots). **b,** the number of antigen-specific memory B cells cross-reactive with both WT and K417N/E484K/N501Y (KEN) RBD mutant per 10 million B cells after prime or boost

303 (n=26), **c,** the frequency of IgM, IgG, or IgA isotype expression by Wuhan-Hu RBD-specific
304 memory B cells after prime or boost (n=10), and **d,** number of Wuhan-Hu RBD-binding
305 plasmablasts per 10 million B cells (n=26) after prime or boost. Red numbers indicate geometric
306 means. Gating strategy is in Extended Data Fig. 2. **e-f,** Pie charts show the distribution of IgG
307 antibody sequences obtained from memory B cells from 11 individuals after **e,** prime or boost or
308 5-months, and **f,** 2- or 5- months. The number inside the circle indicates the number of sequences
309 analyzed for the individual denoted above the circle, with Pfizer vaccinees indicated by (P) and
310 Moderna by (M). Invidiuals in red text indicate those that were sampled at prime, boost, and again
311 5 months post-vaccination. Pie slice size is proportional to the number of clonally related
312 sequences. The black outline and associated numbers indicate the percentage of clonally expanded
313 sequences detected at each time point. Colored slices indicate persisting clones (same IGHV and
314 IGLV genes, with highly similar CDR3s) found at more than one timepoint within the same
315 individual. Grey slices indicate clones unique to the timepoint. White slices indicate repeating
316 sequences isolated only once per time point. **g,** Graph shows the relative percentage of expanded
317 clonal sequences at each time point in **e** and **f**. The red numbers indicate the geometric means. **h,**
318 Number of nucleotide mutations in the IGVH and IGVL combined (also Supplementary Table 4)
319 in the antibodies illustrated in **e** and **f**, compared to the number of mutations obtained after 1.3[3] or
320 6.2[7] months after infection (illustrated by grey dots)**.** Red horizontal bars and numbers indicate
321 mean number of nucleotide mutations at each time point. Statistical significance in **a-d** and **g** was
322 determined using Wilcoxon matched-pairs signed rank test. Statistical significance in **h** was
323 determined by Kruskal Wallis test with subsequent Dunn's multiple comparisons.
324

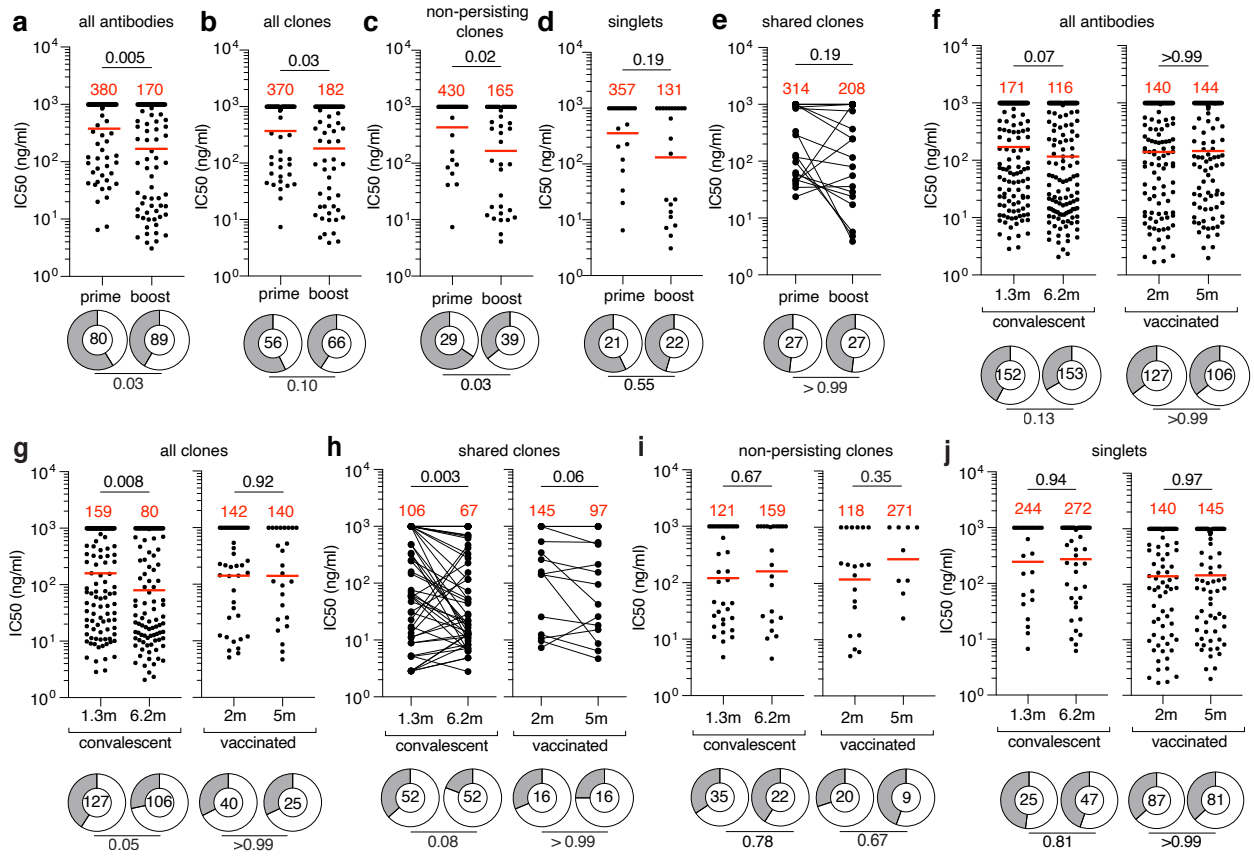

Fig. 3: Anti-SARS-CoV-2 RBD monoclonal antibodies. a-j, Graphs show anti-SARS-CoV-2 neutralizing activity of monoclonal antibodies measured by a SARS-CoV-2 pseudotype virus neutralization assay using wild-type (Wuhan Hu-1[47]) SARS-CoV-2 pseudovirus[3,8]. **a-e,** Half-maximal inhibitory concentration (IC_{50}) values for all antibodies (**a**), all clones (**b**), non-persisting clones (**c**), singlets (**d**) and shared clones (**e**) isolated after prime or boost. **f-j**, Half-maximal inhibitory concentration (IC_{50}) values for all antibodies (**f**), all clones (**g**), shared clones (**h**), non-persisting clones (**i**) and singlets (**j**) isolated from COVID-19 convalescent individuals 1.3[3] and 6.2[7] months after infection or from vaccinated individuals 2m[12] or 5m after vaccination. Each dot represents one antibody. Pie charts illustrate the fraction of non-neutralizing (IC50 > 1000 ng/ml) antibodies (grey slices), inner circle shows the number of antibodies tested per group. Horizontal bars and red numbers indicate geometric mean values. Statistical significance in **a-d, f, g, i, j** was

337 determined by Mann-Whitney test and in **e** and **h** by Wilcoxon test. Statistical significance for ring

338 plots was determined using Fisher's exact test. All experiments were performed at least twice.

339

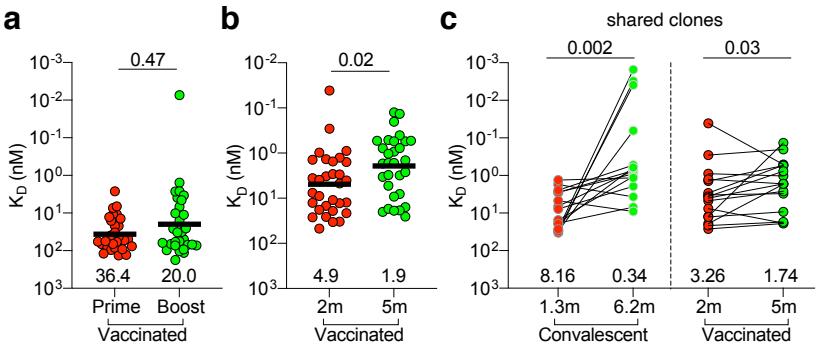

d Vaccination persisting clones 2m/5m

	wt	R683G	R346S	K417N	N440K	A475V	E484K R683G	Q493R	N501Y	KEN R683G	L452R E484Q R683G	L452R T478K R683G
C1332	5	4	8	7	6	5	5	6	5	4	4	5
C1207	103	68	121	86	125	19	61	58	26	3	61	61
C1189	113	103	129	6	112	78	5	80	77	73	8	76
C1213	101	101	14	178	164	148	52	132	133	48	100	100
C1344	77	13	77	96	66	100	93	50	82	78	78	83
C1335	48	79	73	54	68	48	86	64	50	61	141	105
C1333	86	99	97	87	89	84	95	109	93	88	92	114
C1334	65	107	173	88	109	82	99	95	66	79	112	111
C1211	115	113	165	109	188	142	122	105	126	125	130	128
C1302	85	21	70	588	64	109	77	97	102	529	78	107

%IC50 of shared clone isolated 2m after vaccination

e Convalescent infection persisting clones 1.3m/6m

	wt	R683G	R346S	K417N	N440K	A475V	E484K R683G	Q493R	N501Y	KEN R683G	L452R E484Q R683G	L452R T478K R683G
C542	2	4	2	1	2	2	1	2	1	13	1	2
C099	3	1	4	2	3	2	1	5	8	0.4	2	1
C513	16	5	19	9	10	4	15	15	15	5	4	2
C573	1	5	100	1	1	1	2	1	2	1	2	4
C043	18	2.9	17	51	13	4	1	0.3	14	2	1	3
C512	10	2	100	2	25	7	0.3	9	53	0.2	1	2
C055	2	1	2	3	2	1	42	1	1	30	1	100
C080	70	69	3	11	4	35	10	68	71	20	1	1
C549	29	6	62	38	46	44	4	1	15	34	0.1	1
C511	83	45	101	34	71	3	24	10	1	0.2	25	23
C057	47	43	38	35	30	30	89	4	22	100	0.1	31
C095	88	19	121	15	44	57	100	0.3	81	100	100	0.2
C502	154	61	169	136	97	124	100	1	126	100	100	1
C572	148	28	96	60	127	138	100	100	401	144	248	184
C051	295	49	525	293	412	241	52	1	419	100	7	34
C052	48	112	37	50	36	35	192	457	27	100	100	41

%IC50 of shared clone isolated 1.3m after infection

Fig. 4: Affinity and Breadth. a-c, Graphs show antibody K_Ds for Wuhan-Hu RBD measured by BLI. **a,** antibodies isolated from vaccinees after prime (red, n=30) or boost (green, n=30). **b**, same as **a,** but from vaccinees after 2- (red, n=31) and 5-months (green, n=30). **c**, Clonal-paired antibodies isolated from convalescents 1.3[3]- and 6[7]-months after infection (n=15) or vaccinated individuals 2- and 5-months after full vaccination (n=16). Black horizontal bars and numbers indicate geometric mean values. Statistical significance was determined using two-tailed unpaired

347 t-test (**a, b**) or two tailed Kruskal Wallis test with subsequent Dunn's multiple comparisons (**c**).
348 BLI traces can be found in Extended Data Fig 7**. d-e,** Heat-maps show inhibitory concentrations
349 of antibodies isolated 5m after vaccination (**d**) or 6.2 months[7] after infection (**e**) normalized to their
350 shared clone isolated 2m after vaccination (**d**) or 1.3 months[3] after infection (**e**), expressed as
351 %IC50, against indicated mutant SARS-CoV-2 pseudoviruses (Supplementary Table 9).
352 Antibodies with improved (<30%) IC50 compared to their clonal relative isolated at an earlier
353 timepoint are colored in shades of green with most improved antibodies in darkest green.
354 Antibodies with worse (>300%) IC50 than their clonal relative isolated at an earlier timepoint are
355 colored in red with the most worsened antibodies in dark red. Antibodies that did not change their
356 IC50 by more than ~3-fold are shown in yellow.
357
358

359 **METHODS**

360

361 **Study participants**.

362 Participants were healthy volunteers receiving either the Moderna (mRNA-1273) or Pfizer-
363 BioNTech (BNT162b2) mRNA vaccines against SARS-CoV-2 who were recruited for serial blood
364 donations at Rockefeller University Hospital in New York between January 21 and June 23, 2021.
365 Participants indicated as "Prime/Boost" were individuals who were *de novo* recruited for this
366 study, while a subgroup of individuals (indicated as "2m/5m") were from a long-term study
367 cohort[12]. Eligible participants were healthy adults with no history of infection with SARS-CoV-2,
368 as determined by clinical history and confirmed through serology testing, receiving one of the two
369 Moderna (mRNA-1273) or Pfizer-BioNTech (BNT162b2), according to current dosing and
370 interval guidelines. Exclusion criteria included incomplete vaccination status, presence of clinical
371 signs and symptoms suggestive of acute infection with or a positive RT-PCR results for SARS-
372 CoV-2 in saliva, or a positive COVID-19 serology. Seronegativity for COVID-19 was established
373 through the absence of serological activity toward the nucleocapsid protein (N) of SARS-CoV-2.
374 Participants presented to the Rockefeller University Hospital for blood sample collection and were
375 asked to provide details of their vaccination regimen, possible side effects, comorbidities and
376 possible COVID-19 history. All participants provided written informed consent before
377 participation in the study and the study was conducted in accordance with Good Clinical Practice.
378 The study was performed in compliance with all relevant ethical regulations and the protocol
379 (DRO-1006) for studies with human participants was approved by the Institutional Review Board
380 of the Rockefeller University. For detailed participant characteristics see Supplementary Tables 1
381 and 2.

382

383 **Blood samples processing and storage.**

384 Peripheral Blood Mononuclear Cells (PBMCs) obtained from samples collected at Rockefeller
385 University were purified as previously reported by gradient centrifugation and stored in liquid
386 nitrogen in the presence of FCS and DMSO[3,7]. Heparinized plasma and serum samples were
387 aliquoted and stored at -20°C or less. Prior to experiments, aliquots of plasma samples were heat-
388 inactivated (56°C for 1 hour) and then stored at 4°C.

389

390 **ELISAs**

391 ELISAs[48,49] to evaluate antibodies binding to SARS-CoV-2 RBD were performed by coating of
392 high-binding 96-half-well plates (Corning 3690) with 50 µl per well of a 1µg/ml protein solution
393 in PBS overnight at 4 °C. Plates were washed 6 times with washing buffer (1× PBS with 0.05%
394 Tween-20 (Sigma-Aldrich)) and incubated with 170 µl per well blocking buffer (1× PBS with
395 2% BSA and 0.05% Tween-20 (Sigma)) for 1 h at room temperature. Immediately after
396 blocking, monoclonal antibodies or plasma samples were added in PBS and incubated for 1 h at
397 room temperature. Plasma samples were assayed at a 1:66 starting dilution and 10 additional
398 threefold serial dilutions. Monoclonal antibodies were tested at 10 µg/ml starting concentration
399 and 10 additional fourfold serial dilutions. Plates were washed 6 times with washing buffer and
400 then incubated with anti-human IgG, IgM or IgA secondary antibody conjugated to horseradish
401 peroxidase (HRP) (Jackson Immuno Research 109-036-088 109-035-129 and Sigma A0295) in
402 blocking buffer at a 1:5,000 dilution (IgM and IgG) or 1:3,000 dilution (IgA). Plates were
403 developed by addition of the HRP substrate, TMB (ThermoFisher) for 10 min (plasma samples)
404 or 4 minutes (monoclonal antibodies). The developing reaction was stopped by adding 50 µl of 1

405 M H_2SO_4 and absorbance was measured at 450 nm with an ELISA microplate reader (FluoStar
406 Omega, BMG Labtech) with Omega and Omega MARS software for analysis. For plasma
407 samples, a positive control (plasma from participant COV72, diluted 66.6-fold and ten additional
408 threefold serial dilutions in PBS) was added to every assay plate for validation. The average of
409 its signal was used for normalization of all the other values on the same plate with Excel
410 software before calculating the area under the curve using Prism V9.1(GraphPad). For
411 monoclonal antibodies, the EC50 was determined using four-parameter nonlinear regression
412 (GraphPad Prism V9.1). EC50s above 2000 ng/mL were considered non-binders.
413
414 **Proteins**
415 Mammalian expression vector encoding the RBD of SARS-CoV-2 (GenBank MN985325.1; S
416 protein residues 319-539) was previously described[50].
417
418 **SARS-CoV-2 pseudotyped reporter virus**
419 A panel of plasmids expressing RBD-mutant SARS-CoV-2 spike proteins in the context of
420 pSARS-CoV-2-S $_{\Delta 19}$ has been described[12,22,51]. Variant pseudoviruses resembling variants of
421 concern B.1.1.7 (first isolated in the UK), B.1.351 (first isolated in South-Africa), B.1.526 (first
422 isolated in New York City), P.1 (first isolated in Brazil) and B.1.617.2 (first isolated in India)
423 were generated by introduction of substitutions using synthetic gene fragments (IDT) or overlap
424 extension PCR mediated mutagenesis and Gibson assembly. Specifically, the variant-specific
425 deletions and substitutions introduced were:
426 B.1.1.7: ΔH69/V70, ΔY144, N501Y, A470D, D614G, P681H, T761I, S982A, D118H
427 B.1.351: D80A, D215G, L242H, R246I, K417N, E484K, N501Y, D614G, A701V

428 B.1.526: L5F, T95I, D253G, E484K, D614G, A701V.

429 P.1: L18F, T20N, P26S, D138Y, R190S, K417T, E484K, N501Y, D614G, H655Y, T1027I,

430 V1167F

431 B.1.617.2: T19R, Δ156-158, L452R, T478K, D614G, P681R, D950N

432 The E484K, K417N/E484K/N501Y (KEN), L452R/E484Q and L452R/T478K substitution, as

433 well as the deletions/substitutions corresponding to variants of concern listed above were

434 incorporated into a spike protein that also includes the R683G substitution, which disrupts the

435 furin cleaveage site and increases particle infectivity. Neutralizing activity against mutant

436 pseudoviruses were compared to a wildtype SARS-CoV-2 spike sequence (NC_045512),

437 carrying R683G where appropriate.

438

439 SARS-CoV-2 pseudotyped particles were generated as previously described[3,8]. Briefly, 293T

440 cells were transfected with pNL4-3ΔEnv-nanoluc and pSARS-CoV-2-$S_{\Delta 19}$, particles were

441 harvested 48 hpt, filtered and stored at -80°C.

442

443 **Pseudotyped virus neutralization assay**

444 Fourfold serially diluted plasma from COVID-19-convalescent individuals or monoclonal

445 antibodies were incubated with SARS-CoV-2 pseudotyped virus for 1 h at 37 °C. The mixture

446 was subsequently incubated with $293T_{Ace2}$ cells[3] (for all WT neutralization assays) or

447 HT1080Ace2 cl14 (for all mutant panels and variant neutralization assays) cells[12] for 48h after

448 which cells were washed with PBS and lysed with Luciferase Cell Culture Lysis 5× reagent

449 (Promega). Nanoluc Luciferase activity in lysates was measured using the Nano-Glo Luciferase

450 Assay System (Promega) with the Glomax Navigator (Promega). The relative luminescence units

451 were normalized to those derived from cells infected with SARS-CoV-2 pseudotyped virus in the
452 absence of plasma or monoclonal antibodies. The half-maximal neutralization titers for plasma
453 (NT_{50}) or half-maximal and 90% inhibitory concentrations for monoclonal antibodies (IC_{50} and
454 IC_{90}) were determined using four-parameter nonlinear regression (least squares regression
455 method without weighting; constraints: top=1, bottom=0) (GraphPad Prism).
456
457 **Biotinylation of viral protein for use in flow cytometry**
458 Purified and Avi-tagged SARS-CoV-2 RBD or SARS-CoV-2 RBD KEN mutant (K417N,
459 E484K, N501Y) was biotinylated using the Biotin-Protein Ligase-BIRA kit according to
460 manufacturer's instructions (Avidity) as described before[3]. Ovalbumin (Sigma, A5503-1G) was
461 biotinylated using the EZ-Link Sulfo-NHS-LC-Biotinylation kit according to the manufacturer's
462 instructions (Thermo Scientific). Biotinylated ovalbumin was conjugated to streptavidin-BV711
463 (BD biosciences, 563262) and RBD to streptavidin-PE (BD Biosciences, 554061) and
464 streptavidin-AF647 (Biolegend, 405237)[3].
465
466 **Flow cytometry and single cell sorting**
467 Single-cell sorting by flow cytometry was described previously[3]. Briefly, peripheral blood
468 mononuclear cells were enriched for B cells by negative selection using a pan-B-cell isolation kit
469 according to the manufacturer's instructions (Miltenyi Biotec, 130-101-638). The enriched B
470 cells were incubated in FACS buffer (1× PBS, 2% FCS, 1 mM EDTA) with the following anti-
471 human antibodies (all at 1:200 dilution): anti-CD20-PECy7 (BD Biosciences, 335793), anti-
472 CD3-APC-eFluro 780 (Invitrogen, 47-0037-41), anti-CD8-APC-eFluor 780 (Invitrogen, 47-
473 0086-42), anti-CD16-APC-eFluor 780 (Invitrogen, 47-0168-41), anti-CD14-APC-eFluor 780

474 (Invitrogen, 47-0149-42), as well as Zombie NIR (BioLegend, 423105) and fluorophore-labelled
475 RBD and ovalbumin (Ova) for 30 min on ice. Single CD3-CD8-CD14-CD16−CD20+Ova−RBD-
476 PE+RBD-AF647+ B cells were sorted into individual wells of 96-well plates containing 4 µl of
477 lysis buffer (0.5× PBS, 10 mM DTT, 3,000 units/ml RNasin Ribonuclease Inhibitors (Promega,
478 N2615) per well using a FACS Aria III and FACSDiva software (Becton Dickinson) for
479 acquisition and FlowJo for analysis. The sorted cells were frozen on dry ice, and then stored at
480 −80 °C or immediately used for subsequent RNA reverse transcription. For plasmablast single-
481 cell sorting, in addition to above antibodies, B cells were also stained with anti-CD19-BV605
482 (Biolegend, 302244), and single CD3-CD8-CD14-CD16-CD19+CD20-Ova-RBD-PE+RBD-
483 AF647+ plasmablasts were sorted as described above. For B cell phenotype analysis, in addition
484 to above antibodies, B cells were also stained with following anti-human antibodies: anti-IgD-
485 BV421 (Biolegend, 348226), anti-CD27-FITC (BD biosciences, 555440), anti-CD19-BV605
486 (Biolegend, 302244), anti-CD71- PerCP-Cy5.5 (Biolegend, 334114), anti- IgG-PECF594 (BD
487 biosciences, 562538), anti-IgM-AF700 (Biolegend, 314538), anti-IgA-Viogreen (Miltenyi
488 Biotec, 130-113-481).
489
490 **Antibody sequencing, cloning and expression**
491 Antibodies were identified and sequenced as described previously[3,52]. In brief, RNA from single
492 cells was reverse-transcribed (SuperScript III Reverse Transcriptase, Invitrogen, 18080-044) and
493 the cDNA was stored at −20 °C or used for subsequent amplification of the variable IGH, IGL
494 and IGK genes by nested PCR and Sanger sequencing. Sequence analysis was performed using
495 MacVector. Amplicons from the first PCR reaction were used as templates for sequence- and

496 ligation-independent cloning into antibody expression vectors. Recombinant monoclonal
497 antibodies were produced and purified as previously described[3].
498
499 **Biolayer interferometry**
500 Biolayer interferometry assays were performed as previously described[3]. Briefly, we used the
501 Octet Red instrument (ForteBio) at 30 °C with shaking at 1,000 r.p.m. Affinity measurement of
502 anti-SARS-CoV-2 IgGs binding were corrected by subtracting the signal obtained from traces
503 performed with IgGs in the absence of WT RBD. The kinetic analysis using protein A biosensor
504 (ForteBio 18-5010) was performed as follows: (1) baseline: 60sec immersion in buffer. (2)
505 loading: 200sec immersion in a solution with IgGs 10 μg/ml. (3) baseline: 200sec immersion in
506 buffer. (4) Association: 300sec immersion in solution with WT RBD at 20, 10 or 5 μg/ml (5)
507 dissociation: 600sec immersion in buffer. Curve fitting was performed using a fast 1:1 binding
508 model and the Data analysis software (ForteBio). Mean KD values were determined by
509 averaging all binding curves that matched the theoretical fit with an R^2 value ≥ 0.8.
510
511 **Computational analyses of antibody sequences**
512 Antibody sequences were trimmed based on quality and annotated using Igblastn v.1.14. with
513 IMGT domain delineation system. Annotation was performed systematically using Change-O
514 toolkit v.0.4.540[53]. Heavy and light chains derived from the same cell were paired, and
515 clonotypes were assigned based on their V and J genes using in-house R and Perl scripts. All
516 scripts and the data used to process antibody sequences are publicly available on GitHub
517 (https://github.com/stratust/igpipeline/tree/igpipeline2_timepoint_v2).
518

519 The frequency distributions of human V genes in anti-SARS-CoV-2 antibodies from this study
520 was compared to 131,284,220 IgH and IgL sequences generated by[54] and downloaded from cAb-
521 Rep[55], a database of human shared BCR clonotypes available at https://cab-
522 rep.c2b2.columbia.edu/. Based on the 112 distinct V genes that make up the 7936 analyzed
523 sequences from Ig repertoire of the 11 participants present in this study, we selected the IgH and
524 IgL sequences from the database that are partially coded by the same V genes and counted them
525 according to the constant region. The frequencies shown in Extended Data Fig. 4 are relative to
526 the source and isotype analyzed. We used the two-sided binomial test to check whether the
527 number of sequences belonging to a specific IgHV or IgLV gene in the repertoire is different
528 according to the frequency of the same IgV gene in the database. Adjusted p-values were
529 calculated using the false discovery rate (FDR) correction. Significant differences are denoted
530 with stars.
531
532 Nucleotide somatic hypermutation and CDR3 length were determined using in-house R and Perl
533 scripts. For somatic hypermutations, IGHV and IGLV nucleotide sequences were aligned against
534 their closest germlines using Igblastn and the number of differences were considered nucleotide
535 mutations. The average number of mutations for V genes was calculated by dividing the sum of
536 all nucleotide mutations across all participants by the number of sequences used for the analysis.
537
538 **Data availability statement:** Data are provided in Supplementary Tables 1-9. The raw
539 sequencing data and computer scripts associated with Figure 2 and Extended Data Fig. 3 have
540 been deposited at Github (https://github.com/stratust/igpipeline/tree/igpipeline2_timepoint_v2).
541 This study also uses data from "A Public Database of Memory and Naive B-Cell Receptor

542 Sequences" (https://doi.org/10.5061/dryad.35ks2), PDB (6VYB and 6NB6) and from "High
543 frequency of shared clonotypes in human B cell receptor repertoires"
544 (https://doi.org/10.1038/s41586-019-0934-8).
545
546 **Code availability statement:** Computer code to process the antibody sequences is available at
547 GitHub (https://github.com/stratust/igpipeline/tree/igpipeline2_timepoint_v2).
548
549
550 **Data presentation**
551 Figures arranged in Adobe Illustrator 2020.
552
553 **Competing interests:** The Rockefeller University has filed a provisional patent application in
554 connection with this work on which M.C.N.is an inventor (US patent 63/021,387). The patent
555 has been licensed by Rockefeller University to Bristol Meyers Squib.
556

557 **Acknowledgments:** We thank all study participants who devoted time to our research; The
558 Rockefeller University Hospital nursing staff and Clinical Research Support Office and nursing
559 staff. Mayu Okawa Frank, Marissa Bergh, and Robert B. Darnell for SARS-CoV-2 saliva PCR
560 testing. Charles M. Rice, and all members of the M.C.N. laboratory for helpful discussions, Maša
561 Jankovic for laboratory support, and Kristie Gordon for technical assistance with cell-sorting
562 experiments. This work was support by NIH grant P01-AI138398-S1 (M.C.N.) and
563 2U19AI111825 (M.C.N.). R37-AI64003 to P.D.B.; R01AI78788 to T.H. F.M. is supported by
564 the Bulgari Women & Science Fellowship in COVID-19 Research. C.G. was supported by the

565 Robert S. Wennett Post-Doctoral Fellowship, in part by the National Center for Advancing
566 Translational Sciences (National Institutes of Health Clinical and Translational Science Award
567 program, grant UL1 TR001866), and by the Shapiro-Silverberg Fund for the Advancement of
568 Translational Research. P.D.B. and M.C.N. are Howard Hughes Medical Institute Investigators.

569

570 **Author Contributions:** P.D.B., T.H., and M.C.N. conceived, designed and analyzed
571 the experiments. M. Caskey and C.G. designed clinical protocols. A.C, F.M., D.S.B., Z.W., S.F.
572 M.A., E.B., J.D.S., I.S., J.D. F.S., F.Z., and T.B.T. carried out experiments. A.G. and M. Cipolla
573 produced antibodies. D.S.B., M.D., M.T., K.G.M., C.G. and M. Caskey recruited participants,
574 executed clinical protocols. T.Y.O. and V.R. performed bioinformatic analysis. A.C., F.M,
575 D.S.B., Z.W., S.F., and M.C.N. wrote the manuscript with input from all co-authors.

576

577

578 **EXTENDED FIGURES**

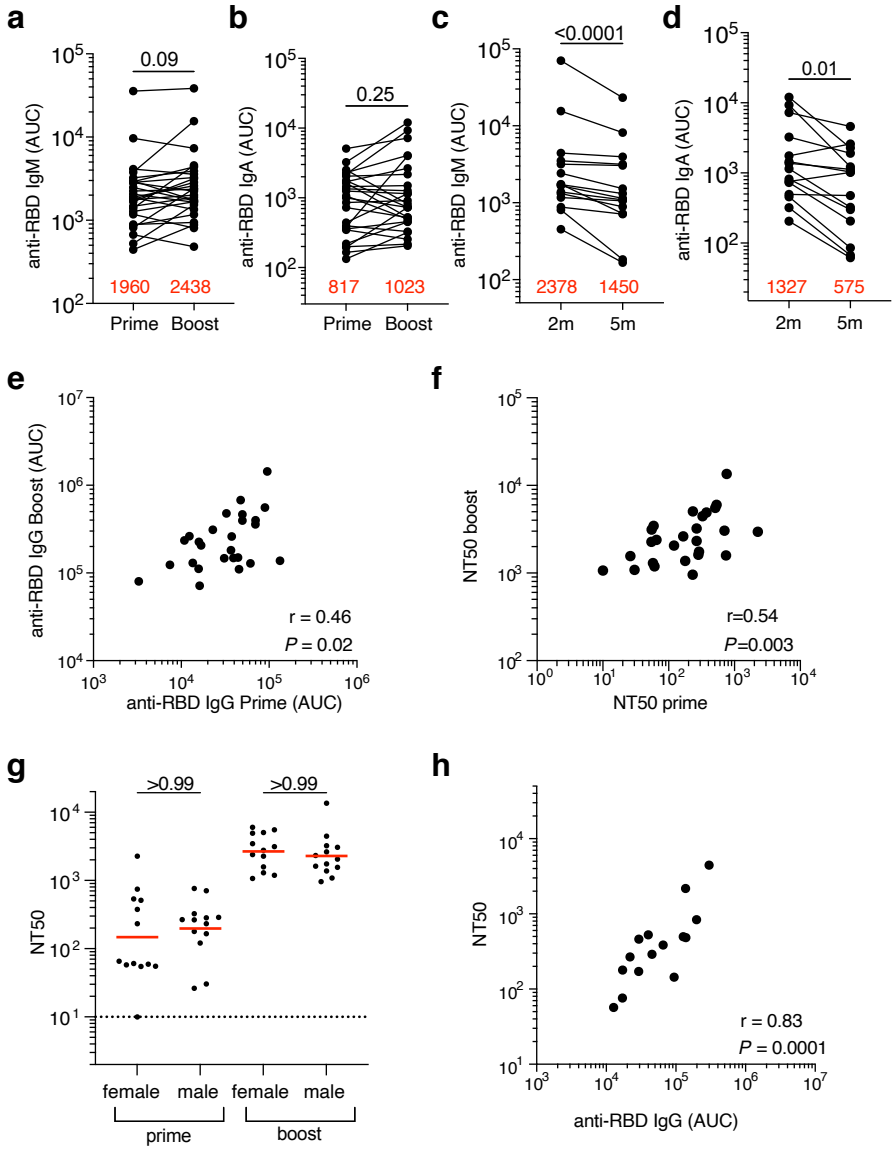

579

580 **Extended Data Fig 1: Plasma ELISA and neutralization.**

581 **a,b,** Graph shows area under the curve (AUC, Y-axis) for plasma IgM (**a**) or IgA (**b**) antibody
582 binding to SARS-CoV-2 RBD after prime and boost for paired samples. **c,d,** Graph shows area
583 under the curve (AUC, Y-axis) for plasma IgM (**c**) or IgA (**d**) antibody binding to SARS-CoV-2
584 RBD of paired samples obtained 2 and 5 months after the boost. **e,f,** IgG antibody binding (AUC,
585 X-axis) after prime vs. IgG antibody binding (AUC, X-axis) after boost (**e**) and NT50 values after

586 prime vs. NT50 values after boost (**f**) in individuals receiving two doses of an mRNA vaccine. **g,**
587 NT50 values after prime and boost in females and males receiving 2 doses of an mRNA vaccine.
588 **h,** NT50 values (Y-axis) vs. IgG antibody binding (AUC, X-axis) 5 months after boost in
589 individuals receiving two doses of an mRNA vaccine. All experiments were performed at least in
590 duplicate. Red values or bar in **a-d** and **g** represent geometric mean values. Statistical significance
591 in **a-d** was determined by Wilcoxon test, in **e, f, and h** by spearman correlation test and in **g** by
592 Kruskall-Wallis test with subsequent Dunn's multiple comparisons.
593

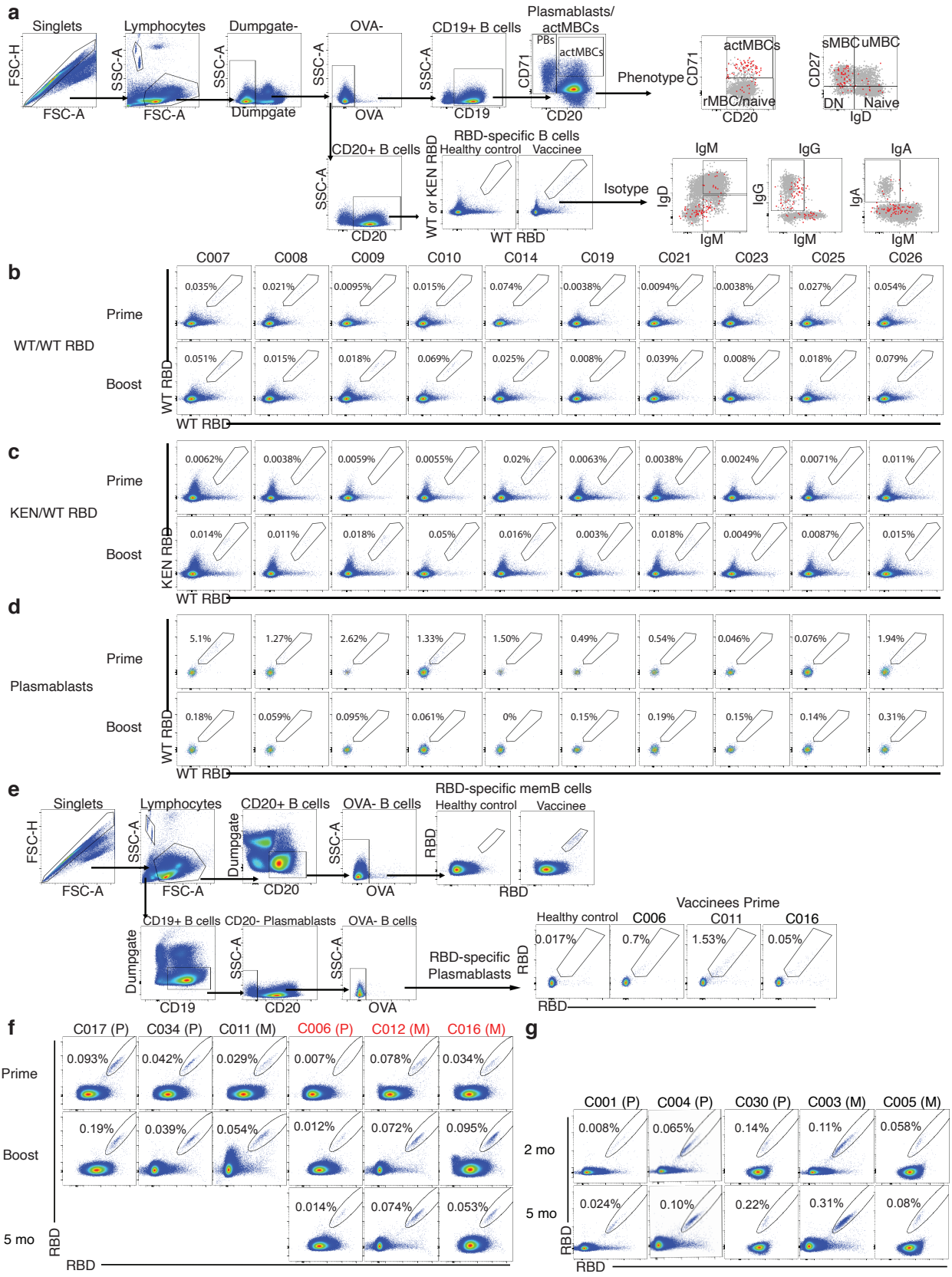
a
Singlets
Lymphocytes
Dumpgate-
OVA-
CD19+ B cells
Plasmablasts/ actMBCs
PBs
actMBCs
Phenotype
actMBCs
rMBC/naive
sMBC
uMBC
DN
Naive
CD20+ B cells
RBD-specific B cells
Healthy control
Vaccinee
Isotype
IgM
IgG
IgA
b
C007
C008
C009
C010
C014
C019
C021
C023
C025
C026
WT/WT RBD
Prime
Boost
c
KEN/WT RBD
d
Plasmablasts
e
RBD-specific memB cells
CD19+ B cells
CD20- Plasmablasts
OVA- B cells
RBD-specific Plasmablasts
Vaccinees Prime
C006
C011
C016
f
C017 (P)
C034 (P)
C011 (M)
C006 (P)
C012 (M)
C016 (M)
5 mo
g
C001 (P)
C004 (P)
C030 (P)
C003 (M)
C005 (M)
2 mo

594

595 **Extended Data Fig. 2: Flow Cytometry. a,** Gating strategy for phenotyping. Gating was on
596 singlets that were $CD19^+$ or $CD20^+$ and CD3-CD8-CD16-Ova-. Anti-IgG, IgM, IgA, IgD, CD71
597 and CD27 antibodies were used for B cell phenotype analysis. Antigen-specific cells were detected
598 based on binding to RBD WT-PE^+ and RBD WT/KEN-$AF647^+$. **b-d,** Flow cytometry plots
599 showing the frequency of **b,** RBD WT-binding memory B cells, and **c,** RBD-binding memory B
600 cells cross-reactive with WT and K417N/E484K/N501Y mutant RBD and **d,** RBD-binding
601 plasmablasts, in 10 selected vaccinees after prime or boost. **e,** Gating strategy for single-cell sorting
602 for CD20+ memory B cells (top panel) or CD19+CD20- plasmablasts (bottom panel) which were
603 double positive for RBD-PE and RBD-AF647. **f-g,** Representative flow cytometry plots showing
604 dual AlexaFluor-647-RBD and PE-RBD-binding, single-cell sorted B cells from **f,** 6 individuals
605 after prime or boost or 5 months post-vaccination and **g,** 5 individuals from 2- or 5-months post-
606 vaccination. Percentage of RBD-specific B cells is indicated. Invidiuals in red text indicate those
607 that were sampled at prime, boost, and again 5 months post-vaccination.
608

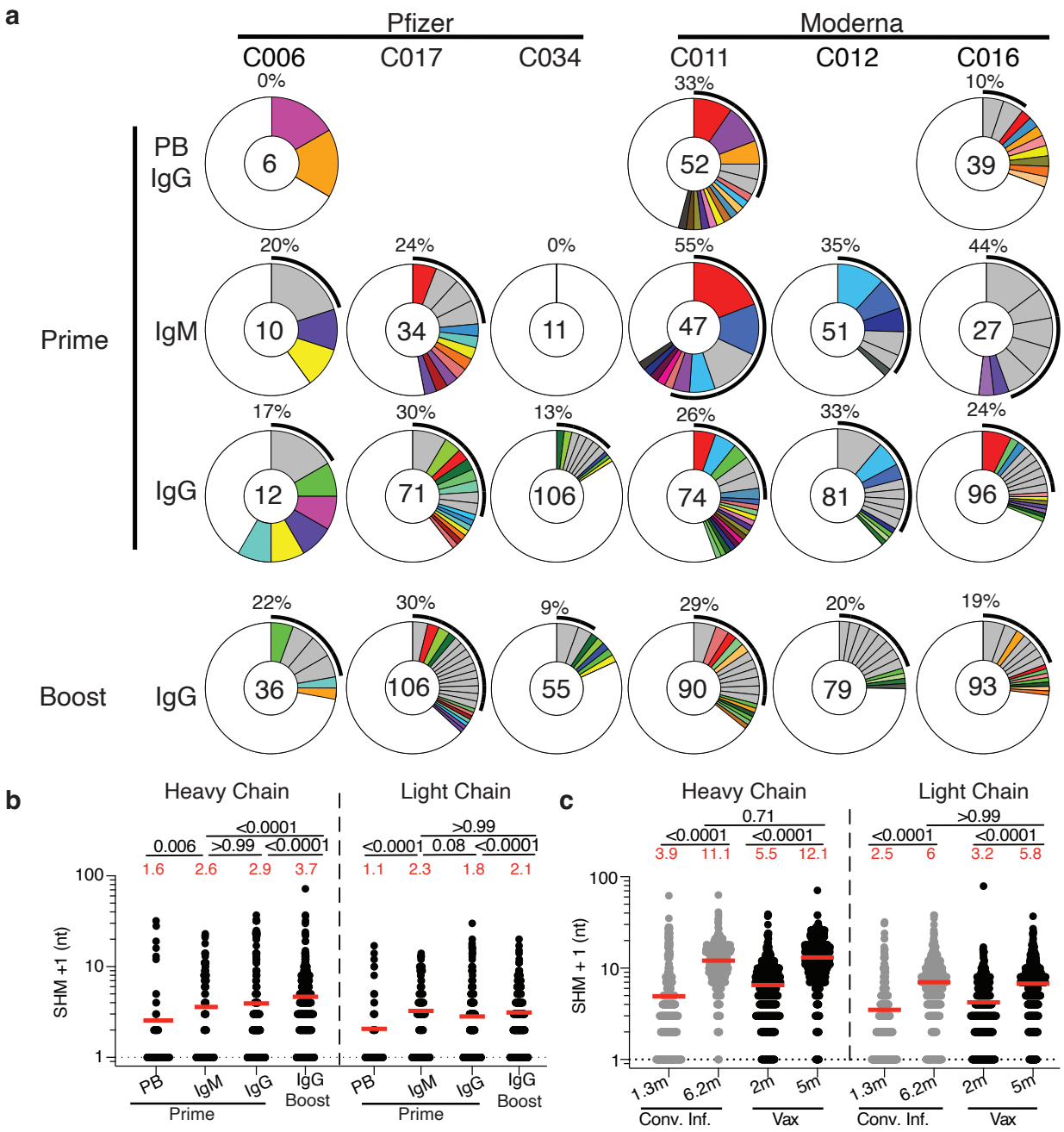

Extended Data Fig 3: anti-SARS-CoV-2 RBD-specific plasmablast and MBC responses after vaccination. a, Pie charts show the distribution of antibody sequences from 6 individuals after prime (upper panel) or boost (lower panel). Sequences derived from IgG plasmablast, IgM MBC, and IgG MBC compartments were analyzed after prime, while only IgG MBCs were analyzed after boost, as indicated to the left of the plots. The number inside the circle indicates the number

615 of sequences analyzed for the individual denoted above the circle. Pie slice size is proportional to
616 the number of clonally related sequences. The black outline indicates the frequency of clonally
617 expanded sequences detected in each patient. Colored slices indicate persisting clones (same IGHV
618 and IGLV genes, with highly similar CDR3s) found in multiple compartments and/or timepoints
619 within the same patient. Grey slices indicate clones unique to the compartment. White indicates
620 sequences isolated once. **b-c,** Number of somatic nucleotide mutations in the IGVH and IGVL,
621 separately, in antibodies detected in **b,** different B cell compartments after prime or boost and **c,**
622 2^{12} or 5 months post-vaccination compared to convalescent infected individuals after 1.3^{3} and 6.2^{7}
623 months post-infection (also Supplementary Table 4). Red horizontal bars and numbers indicate
624 mean number of nucleotide mutations in each compartment at each time point. Statistical
625 significance was determined using a Kruskal Wallis test with subsequent Dunn's multiple
626 comparisons.
627

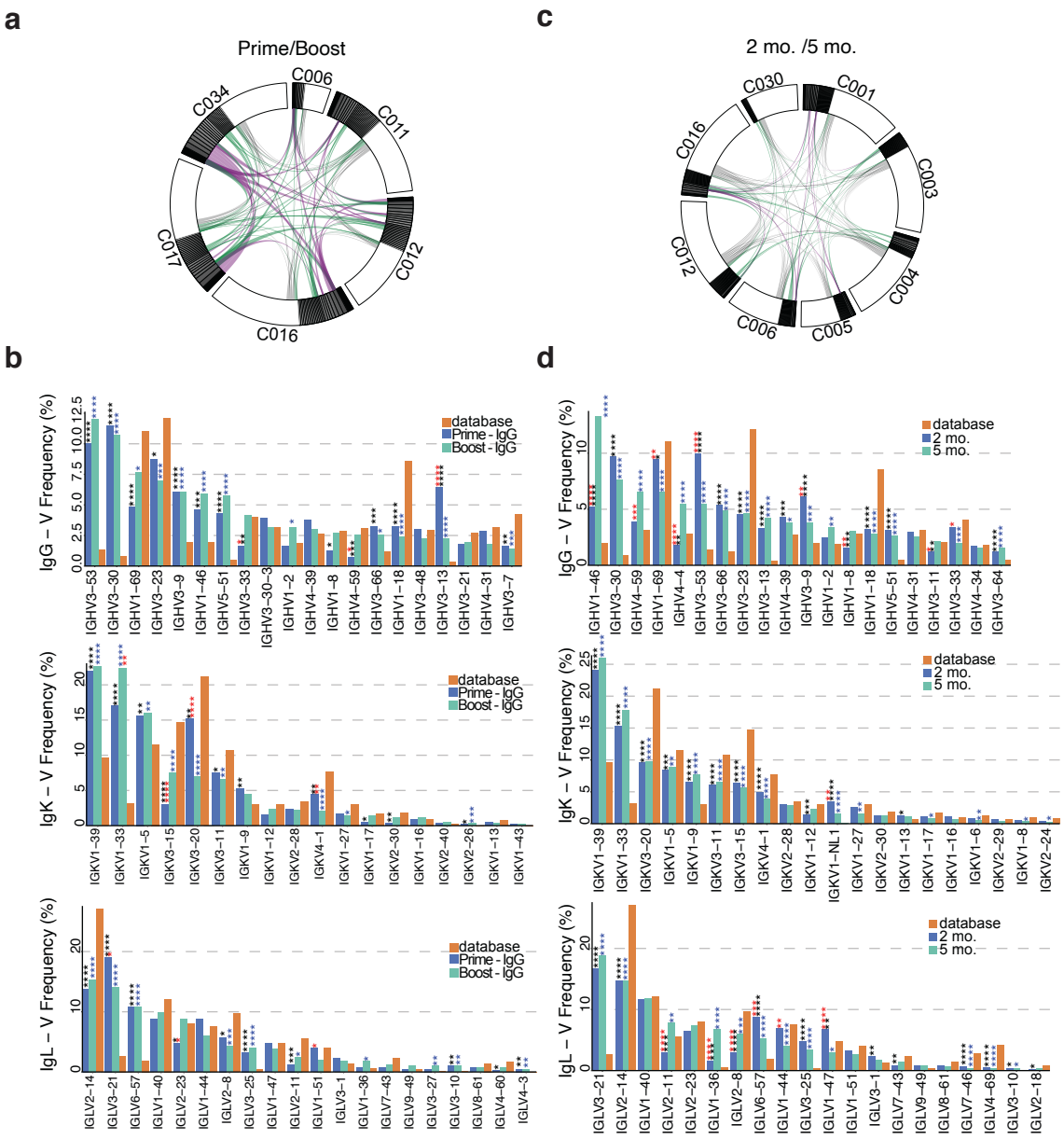

628

629 **Extended Data Fig. 4: Frequency distribution of human V genes. a,** Circos plot depicting
630 relationship between antibodies that share V and J gene usage in both IgH and IgL when comparing
631 all prime/boost IgG MBC sequences. Purple, green, and grey lines connect related clones, clones
632 and singlets, and singlets to each other, respectively. **b,** Graph shows relative abundance of human
633 heavy chain IGVH (top), light chain IGVK (middle) or IGVL (bottom) genes comparing Sequence
634 Read Archive accession SRP010970 (orange), and IgG MBCs after prime (blue) or boost (green)

635 doses of vaccination. Statistical significance was determined by two-sided binomial test. * =
636 $p \leq 0.05$, ** = $p \leq 0.01$, *** = $p \leq 0.001$, **** = $p \leq 0.0001$. Color of stars indicates: black - comparing
637 Database versus Prime; blue - comparing Database versus Boost; red - comparing Prime versus
638 Boost. **c,** Circos plot depicting relationship between antibodies that share V and J gene usage in
639 both IgH and IgL when comparing 2 mo/5 mo IgG MBC sequences. Purple, green, and grey lines
640 connect related clones, clones and singlets, and singlets to each other, respectively. **d,** Graph shows
641 relative abundance of human heavy chain IGVH (top), light chain IGVK (middle) or IGVL
642 (bottom) genes comparing Sequence Read Archive accession SRP010970 (orange), and IgG
643 MBCs after 2 months (blue) or 5 months (green) post-vaccination. Statistical significance was
644 determined by two-sided binomial test. * = $p \leq 0.05$, ** = $p \leq 0.01$, *** = $p \leq 0.001$, **** = $p \leq 0.0001$.
645 Color of stars indicates: black - comparing Database versus 2 months; blue - comparing Database
646 versus 5 months; red - comparing 2 months versus 5 months.
647

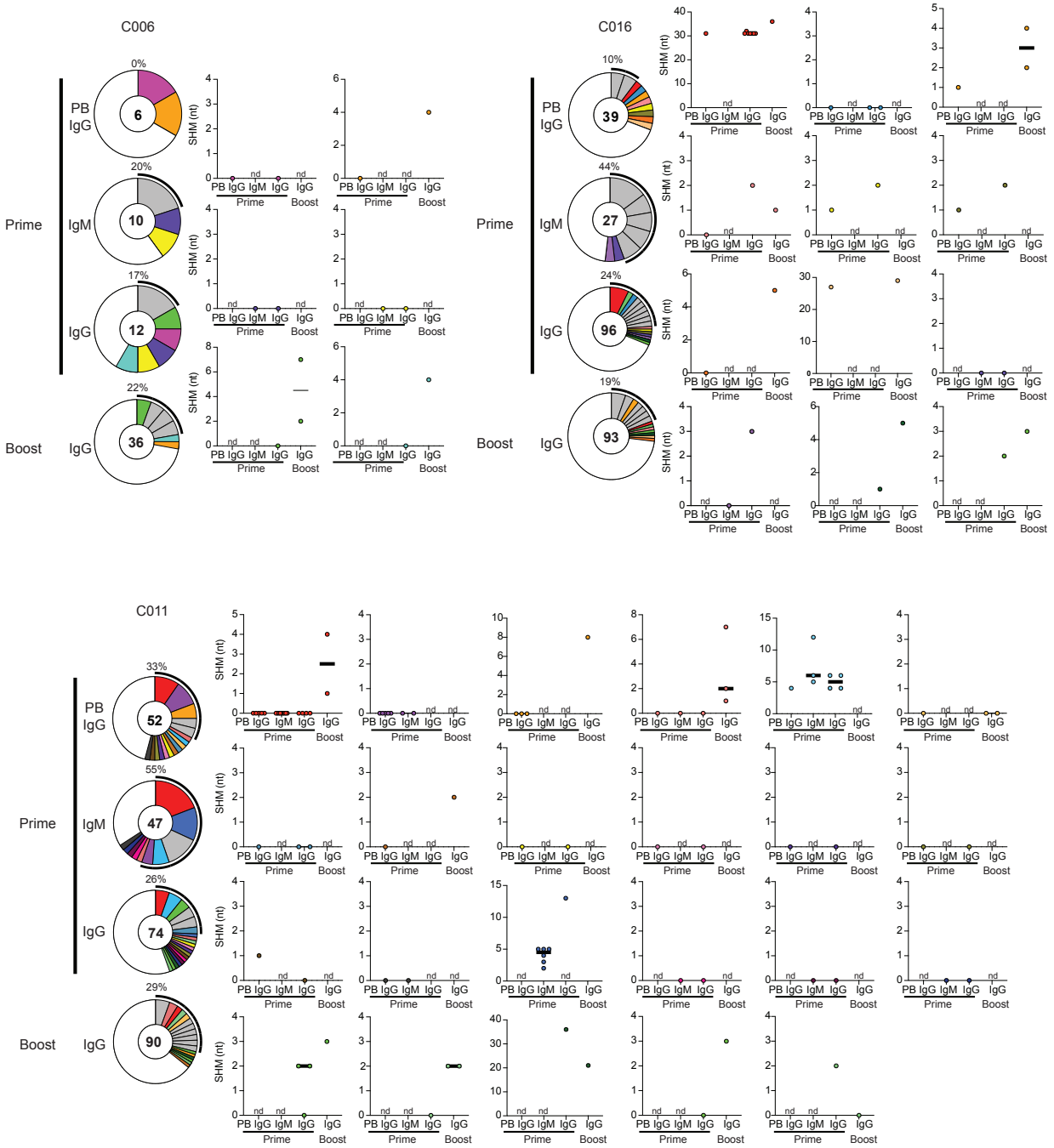

Extended Data Fig. 5: Somatic hypermutation of anti-SARS-CoV-2 RBD antibody clones after prime or boost. Clonal evolution of RBD-binding B cells from 3 individuals for which plasmablasts, IgM memory B cells, and IgG memory B cells were analyzed after prime, and IgG memory B cells were analyzed after boost (as described in Extended Data Fig. 3). The number of

653 somatic nucleotide mutations found in shared clonal families found in at least 2 different
654 compartments is graphed to the right of each donut plot. Color of dot plots match the color of pie
655 slices within the donut plot, which indicate persisting clones. nd – clone was Not Detected in the
656 indicated compartment. Black horizontal line indicates median number of SHM.
657

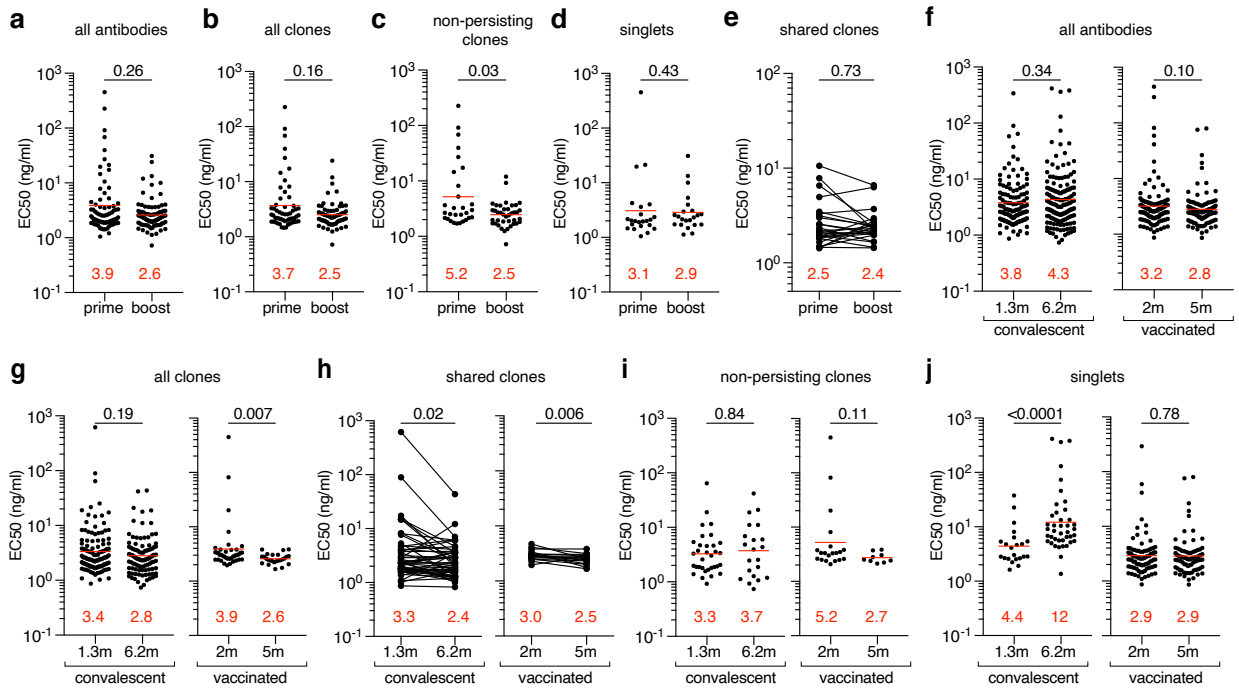

Extended Data Fig. 6: Anti-SARS-CoV-2 RBD monoclonal antibodies ELISAs. a-j, Graphs show anti-SARS-CoV-2 binding activity of monoclonal antibodies measured by ELISA against RBD. **a-e,** ELISA half-maximal concentration (EC_{50}) values for all antibodies (**a**), all clones (**b**), non-persisting clones (**c**), singlets (**d**) and shared clones (**e**) isolated after prime or boost. **f-j**, ELISA half-maximal concentration (EC_{50}) values for all antibodies (**f**), all clones (**g**), shared clones (**h**), non-persisting clones (**i**) and singlets (**j**) isolated from COVID-19 convalescent individuals 1.3[3] and 6.2[7] months after infection or from vaccinated individuals 2m[12] or 5m after vaccination. Each dot represents one antibody. Red horizontal bars and numbers indicate geometric mean values. Statistical significance in **a-d, f, g, i, j** was determined by Mann-Whitney test and in **e** and **h** by Wilcoxon test. All experiments were performed at least twice.

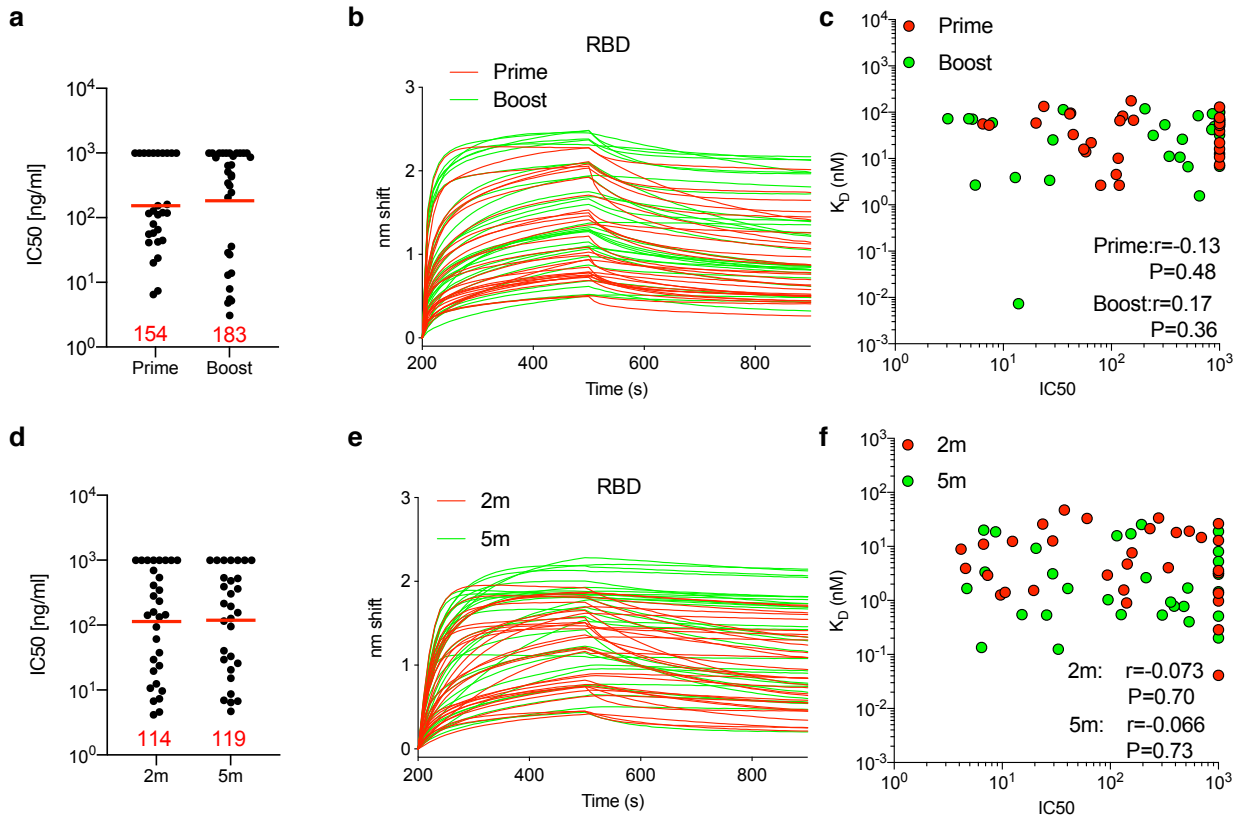

Extended Data Fig. 7. Affinity. Biolayer interferometry measurements. **a**, IC50 values for randomly selected antibodies isolated from vaccinees after prime (n=30) of boost (n=30). Red horizontal lines and numbers indicate geometric mean. **b,** Graphs depict affinity measurements of antibodies described in **a. c,** Graphs show affinities (Y axis) plotted against neutralization activity (X axis) for antibody isolated after vaccination. **d-f,** same as in **a-c,** but showing monoclonal antibodies isolated from follow-up of 2 and 5 months post-vaccination. **d,** IC50 values for randomly selected antibodies isolated from vaccinees after 2- (n=31) or 5- (n=30) months post-vaccination. **e**, Graphs depicting affinity measurements of antibodies described in **d. f,** Graph shows affinity (Y axis) plotted against neutralization activity (X axis) for antibody isolated after vaccination.

a

Prime	wt	R683G	R346S	K417N	N440K	A475V	E484K R683G	Q493R	N501Y	KEN R683G	L452R E484Q R683G
C2159	12.2	6.2	9.1	3.3	11.2	8.8	627.1	17.1	20.6	212.0	36.9
C2029	25.1	7.6	>1000	5.9	23.0	19.5	1.8	14.6	57.7	1.6	>1000
C2139	46.0	25.4	33.0	>1000	48.7	>1000	153.6	>1000	>1000	>1000	105.1
C2033	46.2	25.8	32.0	>1000	41.4	868.4	79.5	183.4	668.2	>1000	52.1
C2209	52.6	26.7	40.7	12.5	48.2	214.0	107.3	341.9	214.9	58.8	44.0
C2020	65.8	37.8	164.0	>1000	53.5	71.5	131.3	>1000	119.0	>1000	83.7
C2221	69.3	26.4	47.6	>1000	58.8	>1000	355.2	>1000	46.3	>1000	124.0
C2019	88.5	96.3	>1000	25.5	90.8	70.1	726.4	92.3	125.5	380.3	>1000
C2110	118.4	106.6	92.6	>1000	109.9	797.4	254.9	198.0	301.5	>1000	218.3
C2018	118.9	37.2	55.4	33.4	110.8	98.0	284.5	123.8	135.8	140.0	>1000
C2022	153.4	61.6	114.5	>1000	130.5	>1000	247.7	358.7	162.8	>1000	139.2
C2113	348.4	127.8	242.4	166.8	267.1	347.9	>1000	922.3	339.4	>1000	>1000
C2149	376.8	178.6	259.3	>1000	331.2	>1000	724.8	>1000	>1000	>1000	608.0
C2026	433.1	25.6	258.1	400.1	350.5	925.7	188.0	368.0	387.1	190.1	147.3
C2150	591.0	57.5	672.9	496.9	413.7	783.8	240.8	406.4	543.2	202.1	199.1
C2013	593.3	204.6	391.0	>1000	484.3	117.9	>1000	>1000	>1000	>1000	>1000
C2185	670.6	116.1	440.0	239.1	494.6	818.2	412.8	759.7	485.4	246.7	251.1
C2004	722.5	117.4	529.5	521.1	468.7	>1000	400.1	496.2	928.0	318.2	345.1
C2140	840.9	124.4	706.9	839.5	778.2	>1000	648.7	866.7	815.5	481.7	497.8
C2109	1000.0	198.7	572.6	825.0	336.9	>1000	960.0	762.2	620.2	691.7	464.7

IC50 (ng/ml)

b

Boost	wt	R683G	R346S	K417N	N440K	A475V	E484K R683G	Q493R	N501Y	KEN R683G	L452R E484Q R683G
C2039	1.9	0.5	1.0	0.7	1.2	1.0	>1000	1.4	2.3	>1000	>1000
C2237	6.7	0.7	3.8	2.3	4.7	3.8	342.4	9.1	4.5	815.8	>1000
C2049	10.0	5.2	7.1	319.9	9.6	65.5	10.9	17.5	12.8	>1000	7.2
C2065	11.6	9.8	>1000	4.0	11.1	6.4	387.7	9.6	11.1	123.4	>1000
C2319	13.3	6.3	8.7	>1000	10.2	131.2	7.7	28.4	297.3	>1000	8.5
C2175	17.6	4.9	12.1	5.1	14.2	8.0	506.1	>1000	17.5	347.0	23.5
C2219	20.7	9.8	13.0	5.2	19.4	35.1	>1000	369.6	13.7	>1000	>1000
C2227	48.3	28.5	94.8	20.6	45.0	36.8	>1000	8.7	>1000	>1000	14.3
C2047	49.1	40.4	145.2	>1000	48.8	53.2	168.6	>1000	96.8	>1000	123.4
C2045	52.0	41.2	46.4	>1000	61.1	375.8	62.9	>1000	60.3	>1000	76.4
C2188	90.8	45.7	64.3	>1000	56.6	743.4	134.8	>1000	>1000	>1000	119.6
C2037	148.1	74.1	53.1	32.7	88.0	103.4	378.3	147.5	157.4	246.4	>1000
C2228	178.4	145.9	124.1	70.2	132.2	>1000	770.5	>1000	197.9	886.3	785.3
C2167	200.4	140.1	156.4	13.6	144.2	143.0	287.9	233.5	183.3	28.4	243.6
C2318	351.9	126.5	262.1	113.7	241.7	335.9	286.4	311.0	477.8	244.8	231.4
C2210	366.2	145.7	236.9	188.6	270.5	297.1	382.6	333.2	276.1	381.7	363.0
C2317	429.2	549.9	>1000	105.5	296.6	282.1	>1000	305.6	387.5	>1000	>1000
C2172	451.6	246.0	324.0	214.0	257.3	>1000	363.5	>1000	486.9	>1000	199.7
C2070	584.0	532.7	856.2	260.7	529.0	709.6	884.3	629.7	802.5	838.8	578.2
C2321	843.9	254.3	>1000	648.9	>1000	627.1	400.1	316.5	693.4	445.2	>1000

IC50 (ng/ml)

Extended data Fig. 8: Breadth of anti-SARS-CoV-2 RBD antibodies elicited after prime and boost vaccination. **a-b**, IC_{50} values for n=40 neutralizing antibodies isolated after prime **(a)** or boost **(b)** against indicated mutant SARS-CoV-2 pseudoviruses. Color gradient indicates IC_{50} values ranging from 0 (white) to 1000 ng/ml (red).

690 **REFERENCES**

691 1 Wang, Z. *et al.* Naturally enhanced neutralizing breadth against SARS-CoV-2 one year
692 after infection. *Nature*, doi:10.1038/s41586-021-03696-9 (2021).
693 2 Goel, R. R. *et al.* Distinct antibody and memory B cell responses in SARS-CoV-2 naive
694 and recovered individuals following mRNA vaccination. *Sci Immunol* **6**,
695 doi:10.1126/sciimmunol.abi6950 (2021).
696 3 Robbiani, D. F. *et al.* Convergent antibody responses to SARS-CoV-2 in convalescent
697 individuals. *Nature* **584**, 437-442, doi:10.1038/s41586-020-2456-9 (2020).
698 4 Apostolidis, S. A. *et al.* Altered cellular and humoral immune responses following
699 SARS-CoV-2 mRNA vaccination in patients with multiple sclerosis on anti-CD20
700 therapy. *medRxiv*, 2021.2006.2023.21259389, doi:10.1101/2021.06.23.21259389 (2021).
701 5 Sokal, A. *et al.* Memory B cells control SARS-CoV-2 variants upon mRNA vaccination
702 of naive and COVID-19 recovered individuals. *bioRxiv*, 2021.2006.2017.448459,
703 doi:10.1101/2021.06.17.448459 (2021).
704 6 Turner, J. S. *et al.* SARS-CoV-2 mRNA vaccines induce persistent human germinal
705 centre responses. *Nature*, doi:10.1038/s41586-021-03738-2 (2021).
706 7 Gaebler, C. *et al.* Evolution of antibody immunity to SARS-CoV-2. *Nature* **591**, 639-644,
707 doi:10.1038/s41586-021-03207-w (2021).
708 8 Schmidt, F. *et al.* Measuring SARS-CoV-2 neutralizing antibody activity using
709 pseudotyped and chimeric viruses. *J Exp Med* **217**, doi:10.1084/jem.20201181 (2020).
710 9 Pilishvili, T. *et al.* Interim Estimates of Vaccine Effectiveness of Pfizer-BioNTech and
711 Moderna COVID-19 Vaccines Among Health Care Personnel - 33 U.S. Sites, January-
712 March 2021. *MMWR Morb Mortal Wkly Rep* **70**, 753-758,
713 doi:10.15585/mmwr.mm7020e2 (2021).
714 10 Lopez Bernal, J. *et al.* Effectiveness of Covid-19 Vaccines against the B.1.617.2 (Delta)
715 Variant. *N Engl J Med*, doi:10.1056/NEJMoa2108891 (2021).
716 11 Reynolds, C. J. *et al.* Prior SARS-CoV-2 infection rescues B and T cell responses to
717 variants after first vaccine dose. *Science*, doi:10.1126/science.abh1282 (2021).
718 12 Wang, Z. *et al.* mRNA vaccine-elicited antibodies to SARS-CoV-2 and circulating
719 variants. *Nature* **592**, 616-622, doi:10.1038/s41586-021-03324-6 (2021).
720 13 Stamatatos, L. *et al.* mRNA vaccination boosts cross-variant neutralizing antibodies
721 elicited by SARS-CoV-2 infection. *Science*, doi:10.1126/science.abg9175 (2021).
722 14 West, A. P. *et al.* Detection and characterization of the SARS-CoV-2 lineage B.1.526 in
723 New York. *bioRxiv*, doi:10.1101/2021.02.14.431043 (2021).
724 15 Edara, V. V. *et al.* Infection and Vaccine-Induced Neutralizing-Antibody Responses to
725 the SARS-CoV-2 B.1.617 Variants. *N Engl J Med*, doi:10.1056/NEJMc2107799 (2021).
726 16 Planas, D. *et al.* Reduced sensitivity of SARS-CoV-2 variant Delta to antibody
727 neutralization. *Nature*, doi:10.1038/s41586-021-03777-9 (2021).
728 17 Victora, G. D. & Nussenzweig, M. C. Germinal centers. *Annu Rev Immunol* **30**, 429-457,
729 doi:10.1146/annurev-immunol-020711-075032 (2012).
730 18 Brouwer, P. J. M. *et al.* Potent neutralizing antibodies from COVID-19 patients define
731 multiple targets of vulnerability. *Science* **369**, 643-650, doi:10.1126/science.abc5902
732 (2020).

733 19 Kreer, C. *et al.* Longitudinal Isolation of Potent Near-Germline SARS-CoV-2-
734 Neutralizing Antibodies from COVID-19 Patients. *Cell* **182**, 843-854 e812,
735 doi:10.1016/j.cell.2020.06.044 (2020).
736 20 Seydoux, E. *et al.* Analysis of a SARS-CoV-2-Infected Individual Reveals Development
737 of Potent Neutralizing Antibodies with Limited Somatic Mutation. *Immunity* **53**, 98-105
738 e105, doi:10.1016/j.immuni.2020.06.001 (2020).
739 21 Taylor, J. J., Pape, K. A., Steach, H. R. & Jenkins, M. K. Humoral immunity. Apoptosis
740 and antigen affinity limit effector cell differentiation of a single naive B cell. *Science* **347**,
741 784-787, doi:10.1126/science.aaa1342 (2015).
742 22 Muecksch, F. *et al.* Development of potency, breadth and resilience to viral escape
743 mutations in SARS-CoV-2 neutralizing antibodies. *bioRxiv*,
744 doi:10.1101/2021.03.07.434227 (2021).
745 23 Amanna, I. J., Carlson, N. E. & Slifka, M. K. Duration of humoral immunity to common
746 viral and vaccine antigens. *N Engl J Med* **357**, 1903-1915, doi:10.1056/NEJMoa066092
747 (2007).
748 24 Davis, C. W. *et al.* Influenza vaccine-induced human bone marrow plasma cells decline
749 within a year after vaccination. *Science* **370**, 237-241, doi:10.1126/science.aaz8432
750 (2020).
751 25 Halliley, J. L. *et al.* Long-Lived Plasma Cells Are Contained within the CD19(-
752)CD38(hi)CD138(+) Subset in Human Bone Marrow. *Immunity* **43**, 132-145,
753 doi:10.1016/j.immuni.2015.06.016 (2015).
754 26 Slifka, M. K., Antia, R., Whitmire, J. K. & Ahmed, R. Humoral immunity due to long-
755 lived plasma cells. *Immunity* **8**, 363-372, doi:10.1016/s1074-7613(00)80541-5 (1998).
756 27 Dan, J. M. *et al.* Immunological memory to SARS-CoV-2 assessed for up to 8 months
757 after infection. *Science* **371**, doi:10.1126/science.abf4063 (2021).
758 28 Sakharkar, M. *et al.* Prolonged evolution of the human B cell response to SARS-CoV-2
759 infection. *Sci Immunol* **6**, doi:10.1126/sciimmunol.abg6916 (2021).
760 29 Widge, A. T. *et al.* Durability of Responses after SARS-CoV-2 mRNA-1273
761 Vaccination. *N Engl J Med* **384**, 80-82, doi:10.1056/NEJMc2032195 (2021).
762 30 Wajnberg, A. *et al.* Robust neutralizing antibodies to SARS-CoV-2 infection persist for
763 months. *Science* **370**, 1227-1230, doi:10.1126/science.abd7728 (2020).
764 31 Pegu, A. *et al.* Durability of mRNA-1273-induced antibodies against SARS-CoV-2
765 variants. *bioRxiv*, doi:10.1101/2021.05.13.444010 (2021).
766 32 Chen, R. E. *et al.* Resistance of SARS-CoV-2 variants to neutralization by monoclonal
767 and serum-derived polyclonal antibodies. *Nat Med* **27**, 717-726, doi:10.1038/s41591-021-
768 01294-w (2021).
769 33 Abu-Raddad, L. J., Chemaitelly, H., Butt, A. A. & National Study Group for, C.-V.
770 Effectiveness of the BNT162b2 Covid-19 Vaccine against the B.1.1.7 and B.1.351
771 Variants. *N Engl J Med* **385**, 187-189, doi:10.1056/NEJMc2104974 (2021).
772 34 Hacisuleyman, E. *et al.* Vaccine Breakthrough Infections with SARS-CoV-2 Variants. *N*
773 *Engl J Med* **384**, 2212-2218, doi:10.1056/NEJMoa2105000 (2021).
774 35 Lumley, S. F. *et al.* Antibody Status and Incidence of SARS-CoV-2 Infection in Health
775 Care Workers. *N Engl J Med* **384**, 533-540, doi:10.1056/NEJMoa2034545 (2021).
776 36 McHeyzer-Williams, L. J., Milpied, P. J., Okitsu, S. L. & McHeyzer-Williams, M. G.
777 Class-switched memory B cells remodel BCRs within secondary germinal centers. *Nat*
778 *Immunol* **16**, 296-305, doi:10.1038/ni.3095 (2015).

37 Mesin, L. *et al.* Restricted Clonality and Limited Germinal Center Reentry Characterize Memory B Cell Reactivation by Boosting. *Cell* **180**, 92-106 e111, doi:10.1016/j.cell.2019.11.032 (2020).
38 Pape, K. A., Taylor, J. J., Maul, R. W., Gearhart, P. J. & Jenkins, M. K. Different B cell populations mediate early and late memory during an endogenous immune response. *Science* **331**, 1203-1207, doi:10.1126/science.1201730 (2011).
39 Viant, C. *et al.* Antibody Affinity Shapes the Choice between Memory and Germinal Center B Cell Fates. *Cell* **183**, 1298-1311 e1211, doi:10.1016/j.cell.2020.09.063 (2020).
40 Sokal, A. *et al.* Maturation and persistence of the anti-SARS-CoV-2 memory B cell response. *Cell* **184**, 1201-1213 e1214, doi:10.1016/j.cell.2021.01.050 (2021).
41 Feng, L. *et al.* An adenovirus-vectored COVID-19 vaccine confers protection from SARS-COV-2 challenge in rhesus macaques. *Nat Commun* **11**, 4207, doi:10.1038/s41467-020-18077-5 (2020).
42 Hassan, A. O. *et al.* A Single-Dose Intranasal ChAd Vaccine Protects Upper and Lower Respiratory Tracts against SARS-CoV-2. *Cell* **183**, 169-184 e113, doi:10.1016/j.cell.2020.08.026 (2020).
43 Greaney, A. J. *et al.* Antibodies elicited by mRNA-1273 vaccination bind more broadly to the receptor binding domain than do those from SARS-CoV-2 infection. *Sci Transl Med* **13**, doi:10.1126/scitranslmed.abi9915 (2021).
44 Pardi, N. *et al.* Expression kinetics of nucleoside-modified mRNA delivered in lipid nanoparticles to mice by various routes. *J Control Release* **217**, 345-351, doi:10.1016/j.jconrel.2015.08.007 (2015).
45 Wu, K. *et al.* Preliminary Analysis of Safety and Immunogenicity of a SARS-CoV-2 Variant Vaccine Booster. *medRxiv*, 2021.2005.2005.21256716, doi:10.1101/2021.05.05.21256716 (2021).
46 Khoury, D. S. *et al.* Neutralizing antibody levels are highly predictive of immune protection from symptomatic SARS-CoV-2 infection. *Nat Med* **27**, 1205-1211, doi:10.1038/s41591-021-01377-8 (2021).
47 Wu, F. *et al.* A new coronavirus associated with human respiratory disease in China. *Nature* **579**, 265-269, doi:10.1038/s41586-020-2008-3 (2020).
48 Amanat, F. *et al.* A serological assay to detect SARS-CoV-2 seroconversion in humans. *Nat Med* **26**, 1033-1036, doi:10.1038/s41591-020-0913-5 (2020).
49 Grifoni, A. *et al.* Targets of T Cell Responses to SARS-CoV-2 Coronavirus in Humans with COVID-19 Disease and Unexposed Individuals. *Cell* **181**, 1489-1501 e1415, doi:10.1016/j.cell.2020.05.015 (2020).
50 Barnes, C. O. *et al.* Structures of Human Antibodies Bound to SARS-CoV-2 Spike Reveal Common Epitopes and Recurrent Features of Antibodies. *Cell* **182**, 828-842 e816, doi:10.1016/j.cell.2020.06.025 (2020).
51 Weisblum, Y. *et al.* Escape from neutralizing antibodies by SARS-CoV-2 spike protein variants. *Elife* **9**, doi:10.7554/eLife.61312 (2020).
52 Wang, Z. *et al.* Enhanced SARS-CoV-2 neutralization by dimeric IgA. *Sci Transl Med* **13**, doi:10.1126/scitranslmed.abf1555 (2021).
53 Gupta, N. T. *et al.* Change-O: a toolkit for analyzing large-scale B cell immunoglobulin repertoire sequencing data. *Bioinformatics* **31**, 3356-3358, doi:10.1093/bioinformatics/btv359 (2015).

824 54 Soto, C. *et al.* High frequency of shared clonotypes in human B cell receptor repertoires.
825 *Nature* **566**, 398-402, doi:10.1038/s41586-019-0934-8 (2019).
826 55 Guo, Y., Chen, K., Kwong, P. D., Shapiro, L. & Sheng, Z. cAb-Rep: A Database of
827 Curated Antibody Repertoires for Exploring Antibody Diversity and Predicting Antibody
828 Prevalence. *Front Immunol* **10**, 2365, doi:10.3389/fimmu.2019.02365 (2019).
829